Chapter 10
Bismuth-Based Compounds as Visible Light Photocatalyst for Remediation and Water Splitting

Mahboobeh Zargazi and Mohammad Chahkandi

Contents

Abstract Enhancing demand for environmental protection has become an urgent need more than ever. For this purpose, water the most known indispensable essences for survivorship of aboveground organisms should be specifically considered. Today, quality of water as dominant source influence of the animate systems has been endangered by various harmful contamination levels. Accordingly, rescuing approaches and cleaning compounds in safe manner demanding for improvement of the quality of potable and industrial utilizing waters are daily pursued. Different materials of bismuth having layered structures, hybridized orbitals, low band gap, and band positions can be attended because of significant ability of water remediation. At this book chapter, we reviewed the photocatalytic efficiency of Bi−compounds, the heterojunction and Z−scheme composites of them, and the synthetization method. Heterojunction or Z−scheme combinations led to obtain high separation photogenerated electrons−hole and reduction of the recombination rate. Furthermore, type II of heterojunction and Z−scheme connections with other

M. Zargazi (✉)
Department of Chemistry, Faculty of Science, Ferdowsi University of Mashhad, Mashhad, Iran

M. Chahkandi (✉)
Department of Chemistry, Hakim Sabzevari University, Sabzevar, Iran
e-mail: m.chahkandi@hsu.ac.ir

Inamuddin et al. (eds.), *Water Pollution and Remediation: Photocatalysis*, Environmental Chemistry for a Sustainable World 57,
https://doi.org/10.1007/978-3-030-54723-3_10

Bi- or non-Bi compounds was applied as an effective solution to enhance photocatalytic performance. The major points are related to the activity about (1) water remediation and (2) photoelectrochemical water splitting. The presented review tries to demonstrate the high potential of Bi−compounds and Bi−composites for water remediation and hydrogen and oxygen production through redox reactions of water activated by solar light irradiation, respectively.

Keywords Bi−compounds · Photocatalyst · Water splitting · Remediation · Heterojunction · Morphology

10.1 Introduction

Worldwide problem of harmful pollutants has been known as the most challenging issue in view of environmental hygiene, health of human, and living organisms on earth (Schwarzenbach et al. 2010; Mahlambi et al. 2015). Human and living organisms need pure and healthy water and air for surviving. Hence, useful technology of photocatalysis process was done in versatile arena like elimination of organic polluters and produce sustainable energy (Aziz and Sopyan 2010; Patil et al. 2015; Kumar 2017). Photocatalyst process started under light irradiation as excitation source for produce active oxidant species on the surface catalyst for proceeding pollutant degradation. Nowadays, attention of researchers for gaining high degradation efficiency with cost-effective has been drawn to use available, non-expensive, and renewable energies such as light source of natural sunlight. It is well clear that sunlight as most available global source could be applied for photocatalysis process. Sunlight spectrum composed of three regions: UV − region about 5%, visible − region about 53%, and infrared region about 42%. The percentage of sunlight constituents can answer to photocatalysts necessity to get light energies and electron stimulation and move them up from conduction band to valence band (Fig. 10.1). From this view, photocatalysts can be categorized to UV-activated and visible light-activated photocatalysts. UV photocatalysts are composed from the semiconductors with wide band gaps more than 3 eV such as ZrO_2, TiO_2, and ZnO but visible ones own lower band gaps between 2 and 3 eV (Akueus 2012; Alahiane et al. 2014; Reddy et al. 2018). Today, researchers have been focused on the synthesize of visible light photocatalysts to benefit from optimal using of main region of natural sunlight. For this matter, we tried to introduce and describe Bi−compounds as visible light photocatalyst within remediation and splitting of water.

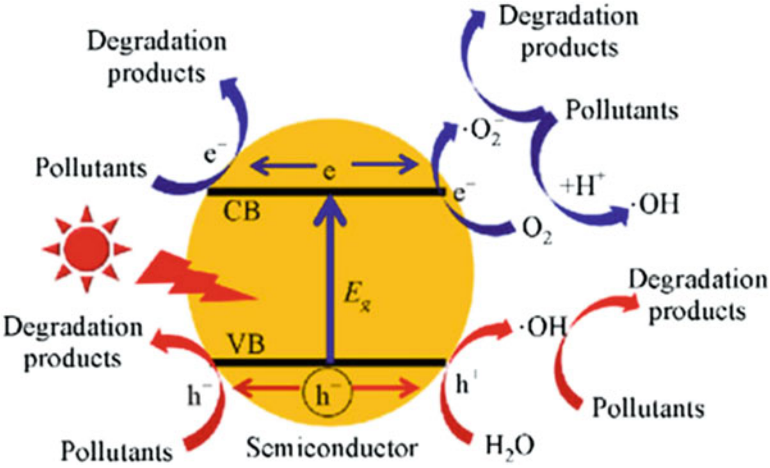

Fig. 10.1 Mechanism of photocatalytic degradation of pollutants over the semiconductor surface. (Reprinted with permission of Springer from Li et al. 2018)

10.2 Photocatalyst Semiconductors

A good photocatalyst should have special properties including (a) sensitive to light, (b) activation under visible or UV light, (c) biological and chemical inert, (d) stable under light without photocorrosion phenomena, (e) affordable, and (f) environmentally safety. To achieve this purpose, vast ranges of semiconductors have been used in photocatalysis process. Effective photocatalysts should produce capability of active radicals ($OH^{•}$, $O_2^{•}$) for oxidation of pollutants which shown in Fig. 10.1. Redox potential of photogenerated valence band holes is positive as enough value ($H_2O/OH^{•}$ = 2.23 eV) to react with adsorbed water molecules to generate hydroxyl radicals. Position of conduction band is sufficient negative for reduction of adsorbed oxygen molecules to produce superoxide radicals. Figure 10.2 shows the various semiconductors including of oxide metals such as TiO_2, ZnO, CuO, SnO_2, WO_3, MnO_2, Bi_2O_3, and Fe_2O_3; chalcogenide metals such as ZnS, MoS_2, WS_2, Bi_2S_3, and FeS; non-metallic such as GO, g-C3N4, and rGO; and mixed metals such as Cu-TiO_2 and Bi-TiO_2 (Opoku et al. 2017). There are different proposed processes to enhance the photocatalytic efficiency, such as preparation of the composites through the elemental modification, heterojunctions with the other semiconductors, and doping with the other elements. Ag and Au metals form could produce plasmonic electrons acting as electron donor for plasmonic nanocomposites (Myung et al. 2014; Alarfaj 2016). Photocatalysts could be interacted with other narrow band gap semiconductors in order to obtain effective heterojunction. Heterojunction helped transferring of charged species between two semiconductors which led to reduce recombination rate of photogenerated electron−hole. Band positions of semiconductors have a key effect at various heterojunctions (Wang

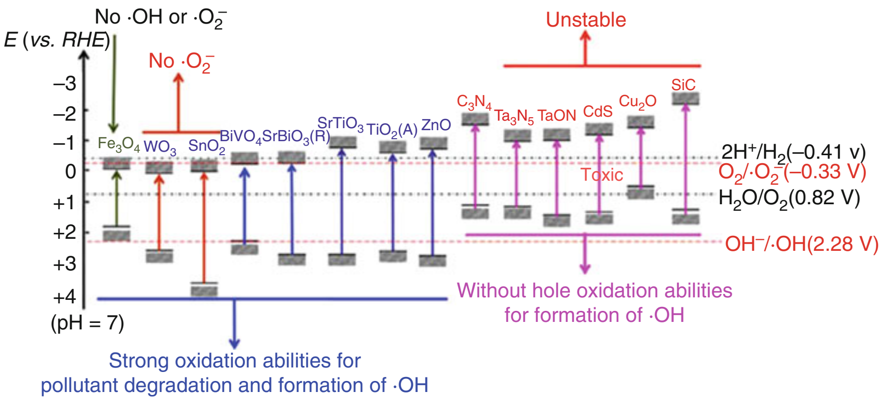

Fig. 10.2 Positions of conduction and valence bands and potentials of typical semiconductors for environmental purifications and capability of them in generation of reactive oxygen species. (Reprinted with permission of Springer from Li et al. 2018)

et al. 2014; Ge et al. 2019). Photocatalysts were used in two forms of powder and film within degradation reactions with some advantages and disadvantages for each of them.

10.2.1 Bi−compounds

Bi−compounds considered as bold visible light-active photocatalysts and have recently drawn rapidly great attention from photocatalyst researchers. Bi^{3+} shows remarkable stability in the different compounds such as Bi_2S_3 (Jin and He 2017), Bi_2WO_6 (Chen et al. 2010), $BiFeO_3$ (Ponraj et al. 2017), $BiVO_4$ (Yin et al. 2010b), $Bi_4Ti_3O_{12}$ (Buscaglia et al. 2011), $BiPO_4$ (Li et al. 2011), $Bi_2O_2CO_3$ (Huang et al. 2015b), and BiOX (X = Cl, Br, I) (Zhang et al. 2008) highly noticed owing to the respected tight band gap, high stability, cost-effective, and environment friendly. Almost all of them have layered structure and sheet like from the view of shape. Although Bi^{5+}−compounds, such as $KBiO_3$ and $NaBiO_3$, can also be activated by visible light, Bi^{5+}−compounds are less considered due to the instability of Bi^{5+} ions. In Bi^{3+} compounds, hybridization of O 2p and Bi 6s orbitals leads to move valence bands to upward states which favor for photocatalytic applications. It can be highlighted that high mobility predicted for photo-induced charge carriers on the Bi−compounds surface due to dispersion of 6s orbitals of bismuth. On the other hand, Bi−compounds have band gaps <3.0 eV that indicate the high activity in visible region. Bi−photocatalysts have interesting capabilities within the environmental issues for removing the organic pollutants such of azo dyes (Zhang et al. 2007; Qin et al. 2012), redox treatments of toxic gases such as NO and CO_2 (Ai et al. 2011a; Jin and He 2017), photoactivated water splitting for H_2 and O_2 evolution reaction. A diverse scientific studies about photocatalytic performance of

Bi−compounds and many other reviewing literature about the photocatalyst field were done (Zhao et al. 2014; Meng and Zhang 2016; He et al. 2018). The present review focused on the photocatalytic activity of various Bi−compounds.

Bi_2X_3

Bi_2X_3 (X = O, S, Se, Te) compounds including Bi and other elements of group VI are generally named bismuth chalcogenides with nomenclature of Bi_2O_3, Bi_2S_3, Bi_2Se_3, and Bi_2T_3. Bi_2O_3, based on the phase structures has different band gap values in the range of 2.1–2.8 eV, causing for consideration as a durable photoactivated by the white light. Bi_2O_3 formed from different polymorph phases which include α, β, δ, γ, and ω with crystal network of monoclinic, tetragonal, body-centered cubic, face-centered cubic, and triclinic, respectively. Various Bi_2O_3 known phases have low stability which lead to quick interphase conversion through switching of the temperature condition. Bi_2O_3 nanostructures have remarkable physicochemical characters such as band gap having low energy, dielectric permittivity, ion conductivity, and photoconductivity which the highlighted properties make Bi_2O_3 as a stable visible light photocatalytic candidates within water splitting and remediation of organic polluters. Recently, controlled synthetization of Bi_2O_3 with specified morphology and certain phase has become a hotspot for photocatalysis researchers. For instance, uniform hierarchical bismuth oxide structures were synthesized and demonstrated excellent visible light activity about degradation of rhodamine B (Zhou et al. 2009). Monoclinic phase of Bi_2O_3 was prepared via calcination of hydrothermal production from $(BiO)_2CO_3$ precursor and indicated excellent photoactivated degradation of NO gas and formaldehyde via visible light radiance (Ai et al. 2011b). Bi_2S_3 was exhibited as a wonderful light-harvesting photocatalyst because of having tight band gap ~1.7 eV and excited in visible and near-IR regions. Bi_2S_3 nanocatalysts have been synthesized in a variety of dimensions of one-directional, e.g., rode in Fig. (10.3a), two-dimensional, e.g., sheet in Fig. 10.3b, and three-dimensional, e.g., urchin-like in Fig. 10.3c by standard

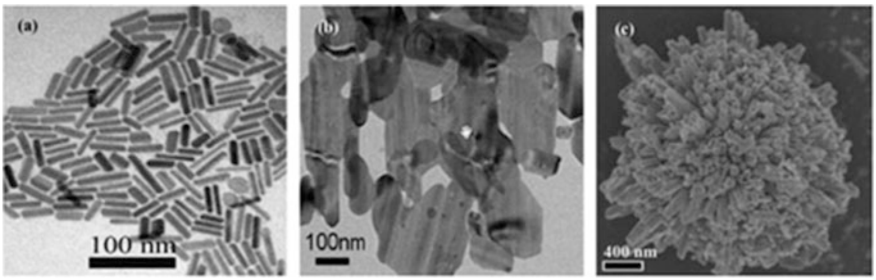

Fig. 10.3 Transmittance electron microscopy images of (**a**) nanorods, (**b**) nanosheets, and (**c**) scanning electron microscopy image of nanospheres of Bi_2S_3. (Reprinted with permission of Springer from Meng and Zhang 2016)

oxygen-free, hot injection, and solvothermal methods, respectively (Wu et al. 2010; Zhang et al. 2011). The photogenerated holes on the Bi_2S_3 semiconductor have efficient energy about 1.62 eV for oxidation of adsorbed water molecules to produce high oxidants such as $OH^{\bullet}$ for degradation of dye contaminants (Zhang et al. 2011). Wu et al. (2010) reported that Bi_2S_3 nanodots and nanorods were synthesized by hot injection method. Uniform Bi_2S_3 nonodots show high photocatalytic degradation for rhodamine B due to the presence of high surface area.

Bi_2Se_3 semiconductor with the layered structure is composed from several monolayers with 0.96 nm thickness that bonded around z−axis with the following configuration Se-Bi-Se-Bi-Se (Sun et al. 2012). Bi_2Se_3 has great potential in photoelectrochemical, optical, and thermoelectrically devices and photocatalysis applications owing to the small band gap and high mobility of charge species (Sun et al. 2012). Bismuth telluride (Bi_2Te_3) also has very narrow band gap about 0.15 eV with trigonal structure and high melting point. Bi_2Te_3 applied in thermoelectric generators and refrigeration due to the thermoelectric properties at 25 °C (Teweldebrhan et al. 2010). Big problem for Bi_2Se_3 and Bi_2Te_3 arrived from the great probability of recombination rate of photogenerated electron−hole pairs that deprives them of the eventual photocatalytic activity.

BiOX

Bismuth oxyhalides represented by BiOX (X = Cl, Br, I) can be considered as the most famous bismuth compounds due to appropriate optical properties and high applications in environment treatment. BiOXs have layered standings similar to other Bi−compounds which characterized by segments of Bi_2O_2 interleaved by double segments of halogens. Layered structures suggested promising large space for polarizing orbitals and created dipoles which could led to separate charge carriers (Lei et al. 2009).

Density functional theory calculation method simulated electrical structures of Bi−oxyhalides (Huang and Zhu 2008). Both the valence band and conduction band of BiOX composed of X np (n = 2–5 for X = F, Cl, Br, and I, respectively), O 2p, and Bi 6p orbitals. The observed band gaps based on computations have resulted as 2.79 eV, 2.34 eV, 1.99, and 1.38 eV for BiOF, BiOCl, BiOBr, and BiOI, respectively (Zhang et al. 2008; Su et al. 2010). Results exhibited that heavy halogen has smaller band gap. So, BiOF as photocatalyst could be excited by UV light, while BiOI activated by visible and near-IR light. It can be stated that BiOBr and BiOCl are repeatedly applied because of the desired amounts of band gaps. The conduction band orbital density isosurfaces are illustrated in Fig. 10.4 for BiOX with the involving of Bi 5d states.

BiOCl is a UV-sensitive photocatalyst with experimental band gap with range of 3.1–3.5 eV and computational calculated band gap of 2.8 eV (Zhang et al. 2006, 2016; Lei et al. 2009). Excited-BiOCl indicated eminent photocatalytic efficiency for pollutant elimination. For instance, Zhang et al. (2006) synthesized durable BiOCl nanoplates via simple hydrolysis method which shown high efficiency about photodegradation of methyl orange activated by UV light. BiOCl nanosheets with

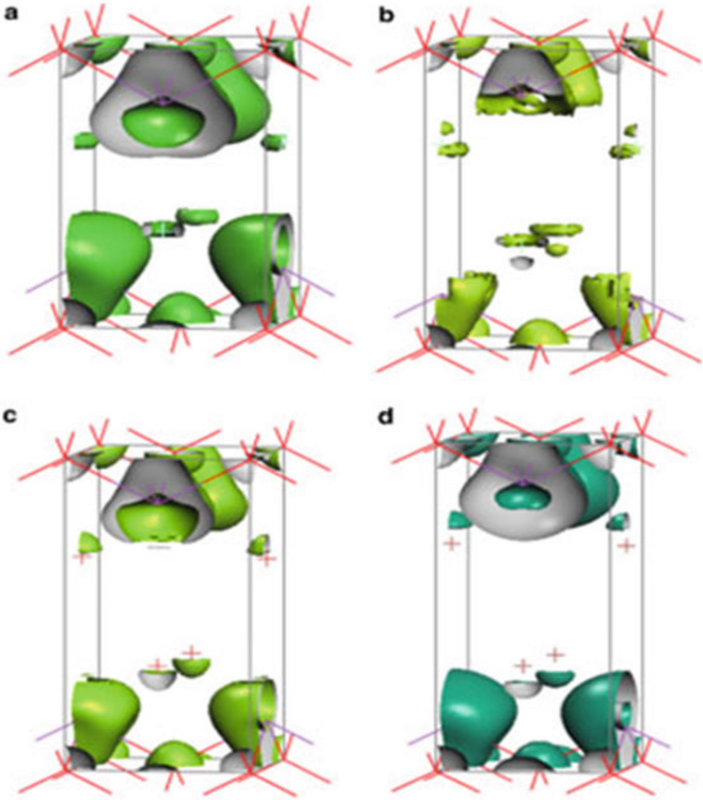

Fig. 10.4 The conduction band orbital density isosurfaces of BiOX (**a**) X = F, (**b**) X = Cl, (**c**) X = Br, and (**d**) X = I with the adoption of Bi 5d states. (Reprinted with permission of Elsevier from Huang and Zhu 2008)

{100} facet could exhibit high photocatalytic activity due to produce oxygen vacancies under UV illumination. In order to make optimum usage of solar energy, there is a remarkable tendency for evaluation of photocatalytic activity of BiOCl under visible light irradiation. If BiOCl coupled with some dyes which have intrinsic physicochemical properties could have visible light activity. For example, Xiong et al. (2011) reported that synthesis of square-like BiOCl nanoplates by hydrothermal method, which has [Cl–Bi–O–Bi–Cl] layered structure and demonstrated high photocatalyst performance for rhodamine B compared to commercial TiO_2 (P25). In this work, diffraction reflectance UV spectroscopy studies for BiOCl nanoplates reported a wide band gap 2.9 eV, so photosensitization process overcome on the photocatalytic process for rhodamine B degradation. At other work, Ye et al. (2012) fabricated marvelous BiOCl with oxygen vacancies under Ar purging, which exhibited 20 times photocatalytic activity than conventional BiOCl for photodegradation of rhodamine B induced via visible light. Porous BiOCl nanosheets also demonstrated photosensitized removal of rhodamine B. Also,

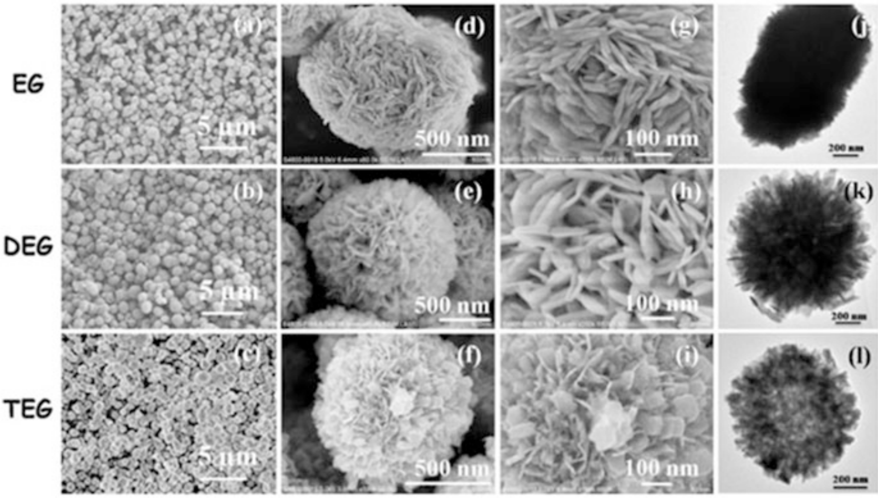

Fig. 10.5 Scanning electron microscopy images (**a**–**i**) and transmittance electron microscopy images (**j**–**l**) of BiOCl nanostructures synthesized via solvothermal method in the presence of polyols: ethylene glycol, diethylene glycol, and triethylene glycol. EG, DEG, and TEG stand for ethylene glycol, diethylene glycol, and triethylene glycol, respectively. (Reprinted with permission of Elsevier from Xiong et al. 2013)

three-dimensional hierarchical BiOCl nanoplates having remarkable photocatalysis efficiency have been successfully prepared. For example, solvothermal with polyol mediator technique was applied for synthesis of specific morphologies BiOCl hierarchical nanostructures. Hierarchical BiOCl (see Fig. 10.5) showed high photoremediation of rhodamine B activated by visible light compared with nanosheets or nanoplates of BiOCl and P25 (Xiong et al. 2013). Unlike BiOCl, BiOBr were introduced as visible light-sensitive semiconductor with inherently appropriate band gap for utilization of sunlight and suggested as a powerful catalyst about photodegradation of organic polluters under white light illumination. Recently, considerable researches have been done to evaluate photocatalytic activity of BiOBr in environmental treatment and photocatalytic water splitting fields. Lamellar and plate-based BiOBr structures were prepared that showed great photocatalyst performance for pollutant degradation (Shang et al. 2009).

BiOBr nanosheets used for photoreduction of Cr(VI) induced by visible light and the reusability indicated high efficiency for reduction process. Researchers have also attracted to synthesize three-dimensional hierarchical BiOBr to enhance the photocatalytic properties which has more advantages in comparison with one-dimensional or two-dimensional structures (Shi et al. 2013). BiOBr with mesoporous structure showed higher visible light photocatalytic efficiency for harmful tetrabromobisphenol A compared to commercial TiO_2. High ranges of pollutants such as dyes, e.g., rhodamine B, methyl orange, methylene blue, and organic, e.g., phenol and toluene have been proposed as mannequin pollutants to exhibit the photocatalyst activity of BiOBr compounds under visible light irradiation

(Zhao et al. 2014). Among BiOX compounds, BiOI has narrowest band gap besides highest utilization of solar source. BiOI is a semiconductor with intrinsic rapid recombination of charge carriers singly, so BiOI cannot show acceptable photocatalytic performance. Therefore, a lot of strategies were proposed for combination/synthetization of BiOI with other semiconductors to improve the related photocatalytic activity.

Bi_2MO_6

Bi_2MO_6 are known as the famous triplet oxygen − bismuth compounds with Aurivillius[1] structure depicted by $(Bi_2O_2)^{2+}(A_{n-1}B_nO_{3n+1})^{2-}$ (A = Ba, Bi, Pb, so on., B = Ti, Nb, W, Mo, so on.) which has intercalated structures with sheets of perovskite-bearing octahedral $(A_{n-1}B_nO_{3n+1})^{2-}$ sandwiched array between $(Bi_2O_2)^{2+}$ layers. Until now, a variety of bismuth Aurivillius oxides containing bismuth tungstate, bismuth molybdate, and bismuth subcarbonate have been fabricated, which has excellent potential for photocatalysis usages such as water treatment and photocatalytic water splitting (Zhao et al. 2014; Meng and Zhang 2016).

Bismuth tungstate (Bi_2WO_6) is known as one of the easiest structures of the Aurivillius group ($n = 1$) having a layered standing with WO_6 sheets. The perovskite block in Bi_2WO_6 composited of 2D array of WO_6 octahedral linked corner, with thick octahedral layer. Bi_2WO_6 has great potential for oxygen evolution reaction within hydrolysis and oxidation of toxic polluters under white light. Zhang et al. (2007) reported that various morphologies of Bi_2WO_6 nano and microstructures, including flower-, tire-, and spiral-like shapes, showed excellent solar light photo-activated catalytic efficiency for remediation of rhodamine B that could be related to the presented morphology, size, and structure. Furthermore, the pH value of the solution contained of pollutant also defines the photocatalytic performance of photocatalyst. Zhu et al. (2016) proved the pH effect of initial solution on the photocatalysis performance of nanosheets Bi_2WO_6 for degradation of rhodamine B which could be related to mode and adsorption−desorption of rhodamine B on the semiconductor surface. Bi_2WO_6 also exhibited high performance for air treatment and water splitting applications (Larson and Zhao 2016). Yu et al. suggested that well-crystalized bismuth tungstate with high surface area which could perform photocatalytic degradation of formaldehyde gas in air (Yu et al. 2005).

Bi_2MoO_6 is also another layered member of Aurivillius compounds which has recently drawn enormous scientific attentions due to the photocatalytic properties within hydrolysis and photooxidation of contaminants. The layered structure Bi_2MoO_6 is synthesized via refluxing method which exhibited high photocatalytic efficiency for oxygen liberation from an aqueous solution of $AgNO_3$ induced by solar light (Shimodaira et al. 2006). The obtained results suggested that

[1]Aurivillius phases are a form of perovskite built by alternating layers of $[Bi_2O_2]^{2+}$ and pseudo-perovskite blocks.

photocatalytic activity attributed to crystallinity and high rate of charge transfer in layered structure Bi_2MoO_6. Zhang et al. (Huang et al. 2018) suggested that nanosheets and microrods of Bi_2MoO_6 were selectively synthesized via change of pH of precursor solution in hydrothermal method and demonstrated efficient visible light photocatalytic degradation of methylene blue. Bi_2MoO_6 has been synthesized via solid state and solvothermal or hydrothermal methods similar to Bi_2WO_6 (Yin et al. 2010a; Zhang et al. 2010). Comparison studies for synthesis method of Bi_2MoO_6 showed that smaller size, large surface area, and efficient photocatalytic performance obtained from samples which fabricated via hydrothermal and solvothermal methods not solid-state reaction. Furthermore, microwave method was also applied to synthesize of Bi_2MoO_6 in short time with good photocatalytic performance (Xie et al. 2008). Different work, thin film of Bi_2MoO_6 (200 nm thickness) fabricated via thermal evaporation deposition process (see Fig. 10.6) which showed high visible light-responsive photocatalyst property for rhodamine B degradation (Cuéllar et al. 2011).

Bismuth titanate, also one important member of Aurivillius oxide family, introduced by a variety of compositions and showed high visible light-sensitive or UV-sensitive photocatalytic for pollutants. Sillenite $Bi_{12}TiO_{20}$ nanowires (Hou et al. 2009) and perovskite $Bi_4Ti_3O_{12}$ (Li et al. 2016) demonstrated high photocatalytic efficiency for methyl orange under light (<400 nm). Cubic phase − Bismuth titanates ($Bi_{12}TiO_{20}$) with a variety of morphological structures such as flower-looking like, belt-looking like, and tetrahedral-looking-like shapes prepared by easy approach showed in Fig. 10.7, which exhibited high photocatalytic degradation performance for methylene orange and *p*-nitrophenol (Guo et al. 2013).

$BiVO_4$

Bismuth vanadate ($BiVO_4$) is known as the most versatile member of Bi−compounds which has three crystallite phases: tetragonal zircon, monoclinic, and tetragonal scheelite structures. $BiVO_4$ with monoclinic crystalline phase became white light photoactivated because of low required energy band gap about 2.4 eV compared to other phases. Hence, $BiVO_4$ with high adsorption in visible light region and narrow band gap was considered as new materials for photocatalytic applications and other related researches. Due to special physicochemical features of $BiVO_4$ such as Ferro elasticity and theoretical band gap about 2.047 eV obtained from density functional theory method, it has been considered as photocatalytic activity, recently (Wang et al. 2019a). Multi shell hollow spheres of $BiVO_4$ synthesized via carbonate template under thermal conditions are depicted in Fig. 10.8. Hollow shapers bear great photo-induced performance within elimination of methylene blue under solar light. Figure 10.9 also confirmed the claimed morphology for $BiVO_4$ with scanning electron microscopy and transmittance electron microscopy images (Zong et al. 2017).

Recently, variety ranges of $BiVO_4$ structures have been synthesized and applied in photocatalytic performances such as elimination of polluters and H_2 or O_2

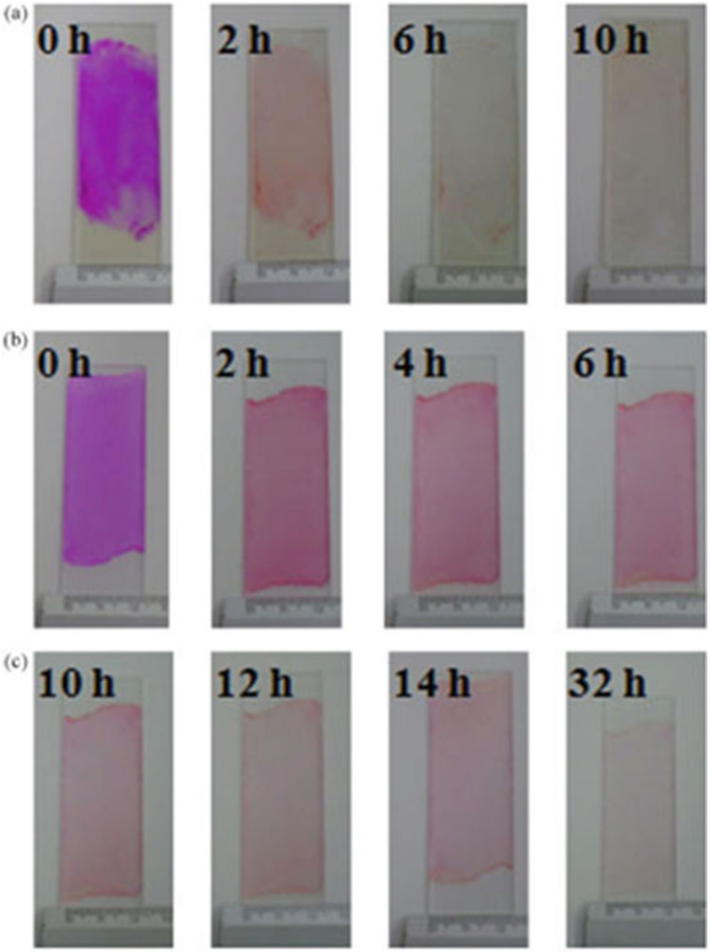

Fig. 10.6 Evaluation of color changing of adsorbed rhodamine B on the Bi_2MoO_6 thin film at different interval time (**a**) and an experiment done on the bare glass (**b** and **c**). (Reprinted with permission of Elsevier from Cuéllar et al. 2011)

liberation from water splitting process (Wang et al. 2019b). Hollow microspheres of $BiVO_4$ showed considerable solar light photocatalysis efficiency for remediation of rhodamine B and 2−propanol (Sun et al. 2013a). At 1998, Kudo's team reported a great candidate with high potential for photocatalytic water splitting named $BiVO_4$ for the first time (Huang et al. 2017). Years later, Kudo et al. demonstrated photoactivated efficiency of bismuth vanadate for O_2 liberation from $AgNO_3$ solution under visible light (Kudo et al. 1999).

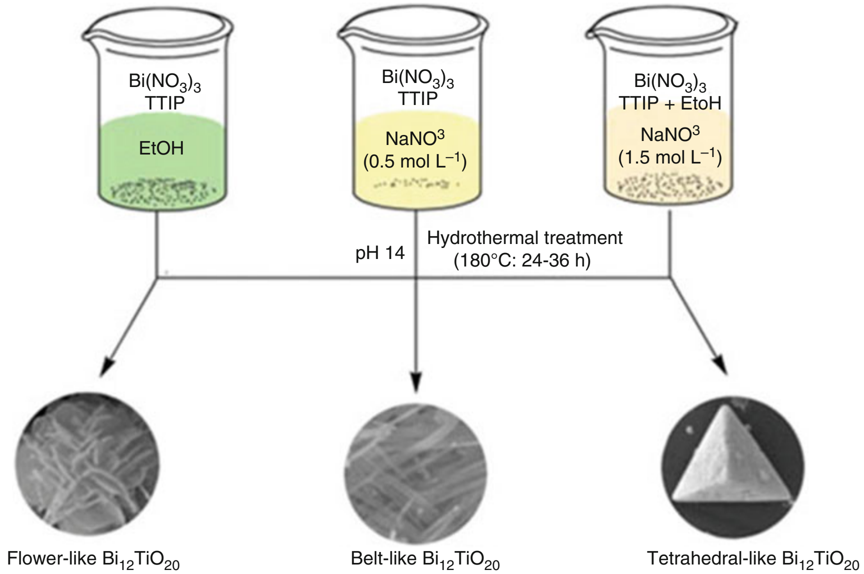

Fig. 10.7 Schematic for fabrication of different morphology for $Bi_{12}TiO_{20}$ by hydrothermal approach. TTIP rephrases for $Ti(OC_3H_7)_4$. (Reprinted with permission of Royal Society of Chemistry from Guo et al. 2013)

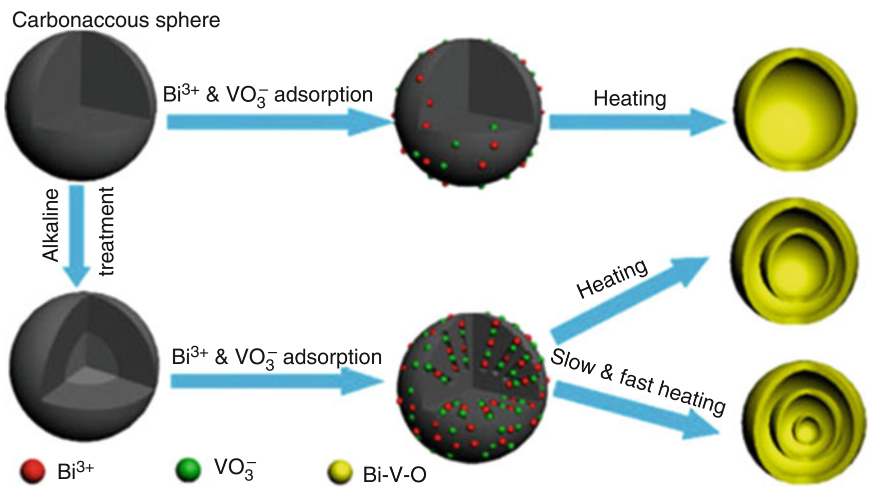

Fig. 10.8 Schematic depicts the fabrication approach of hollow spheres $BiVO_4$. (Reprinted with permission of Elsevier from Zong et al. 2017)

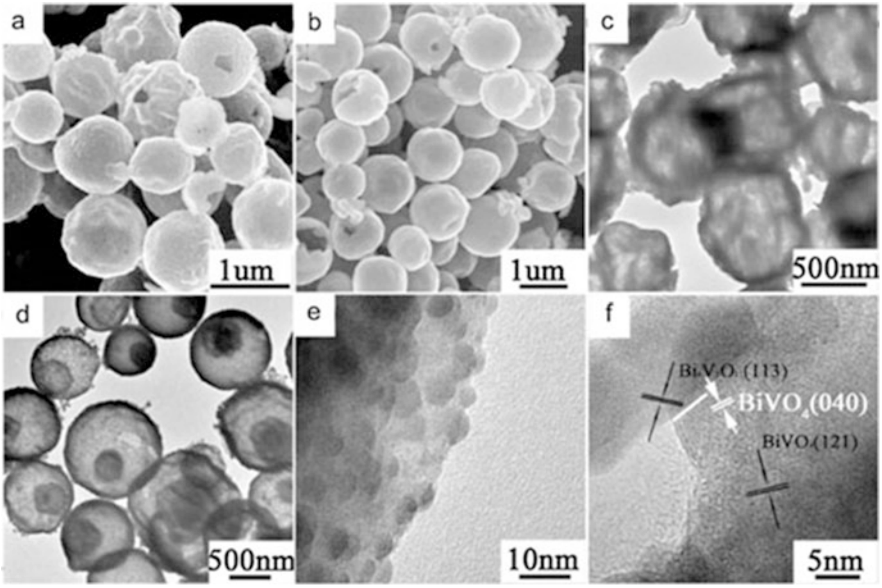

Fig. 10.9 (**a**) Scanning electron microscopy image of Bi–V–O single-shell hollow spheres, (**b**) scanning electron microscopy image of Bi–V–O double−shell hollow spheres, (**c**) transmittance electron microscopy image of Bi–V–O single−shell hollow spheres, (**d**) transmittance electron microscopy image of Bi–V–O double−shell hollow spheres, (**e**) transmittance electron microscopy image of an individual Bi–V–O double−shell hollow spheres, (**f**) high-resolution transmittance electron microscopy image of an individual Bi–V–O double−shell hollow spheres. (Reprinted with permission of Elsevier from Zong et al. 2017)

$BiFeO_3$

$BiFeO_3$ compound shows simultaneous multiferroic and magnetoelectric behaviors at ambient conditions that led to widely employing of $BiFeO_3$ in the arena of nonvolatile memory, spintronic, sensors, and piezoelectric apparatus (Lam et al. 2017; Ponraj et al. 2017). $BiFeO_3$ photocatalyst having rhombohedral disordered perovskite is a new kind of reliable solar light-activated photocatalyst within the organic polluter remediation because of its small band gap and great chemical stability. Last year, $BiFeO_3$ attracted considerable attention in photocatalytic environmental applications (particular degradation dye pollutants such as methylene blue and rhodamine B due to its weak ferromagnetic feature led to recycling from treated solution (Ponraj et al. 2017). Optical band gap of $BiFeO_3$ reported between 2.2 and 2.8 eV in literatures. Mesoporous $BiFeO_3$ hollow sphere was synthesized and used for degradation of rhodamine B and 4−chlorophenol under 500 W Xe-lamp irradiation (Gao et al. 2015). Soltani et al. (Soltani and Entezari 2013a) demonstrated that reactive black 5 bears three main UV/visible peaks at wavelengths of 620, 312, and 254 nm. The generation of some new intermediates such as sulfone, sulfonate, and amine groups prepared in the UV/visible regions is the reason for observation of three main peaks. The residual of small organic intermediates can explain the changing of color solution as well as the decrease of pH.

10.2.2 Modification of Bi−compounds

Although Bi−compounds were introduced as visible light-responsive photocatalyts in water treatment, some compounds such as $BiFeO_3$ and BiOXs have weak adsorption ability which led to poor performance for photocatalytic degradation of pollutants. Relatively poor efficiency can attribute to (i) high recombination rate of electron−hole in bulk or surface, (ii) positions of conduction band or valence band related to O_2 reduction or H_2O oxidation, respectively, and (iii) small surface area for photocatalytic process. So far, many researches were devised for resolving the problematic issues such as morphology modifications, doping, and heterojunctions (Chen et al. 2016a) with other semiconductors and generation of vacancies over the surface. Applying the solutions, either the recombination rate or light harvesting can be effectively decreased or increased, respectively, which led to high performance. For more clearance, follow the more detailed discussion below.

Morphology Control

The chemophysical properties of semiconductors could be changed by main structural factors, size, morphology, and defects, respectively. Subsequently, photocatalytic properties of catalysts can improve by the structural parameters. In this section, we are focused on morphology control of Bi−compounds and investigated photocatalytic performance. Morphology studies were shown improved photocatalytic efficiency because of produce low-dimensional or hierarchical structures, which could create reactive sites, high rate of mass transfer, and more harvesting amount of visible light. In the following, some more innovative producting techniques of low-dimensional and hierarchical structures of Bi−compounds were discussed.

Bi-compounds with Low-Dimensional Structure

Nanomaterials have multifarious dimensions which could be classified to four categories: zero-dimension such as nanoparticles, one-dimension such as nanorods and nanowires, two-dimension such as nanoplates or nanosheets, and three-dimension such as nanospheres or nanoflowers (Jeevanandam et al. 2018). At the recent years, Bi−compounds were synthesized by control of synthetization parameters to obtain special size including nanoparticles, nanobelts, and nanoflowers for photocatalytic applications. Soltani et al. (Soltani and Entezari 2013b, c) reported that $BiFeO_3$ nanoparticles synthesized via ultrasound with narrow size distribution

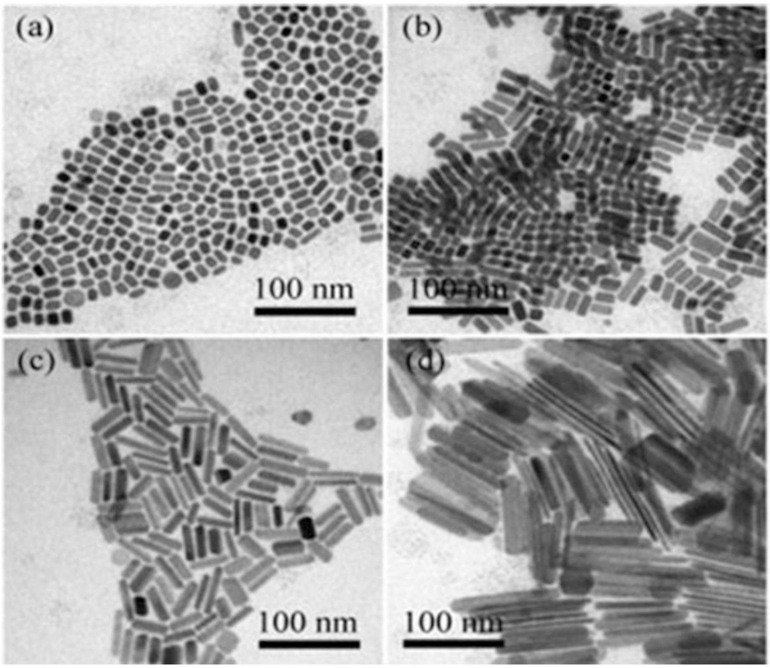

Fig. 10.10 Transmittance electron microscopy images of synthesized Bi_2S_3 nanostructures with various concentrations of Bi (**a**)1:0.5, (**b**) 1:1, (**c**) 1:1.5, and (**d**) 1:1.7. (Zong et al. 2017). (Modified)

as visible light photocatalyst which exhibited higher photocatalytic performance for methylene blue and rhodamine B compared to $BiFeO_3$ synthesized by sol−gel method. Nanodots, nanorods, and nanosheets of Bi_2S_3 nanostructures synthesized and used for degradation of rhodamine B, methylene blue, and methyl orange which results pointed to photocatalytic activity depends to dimension (see Fig. 10.10) (Wu et al. 2010).

The properties of size and porosity of snow-like Bi_2WO_6 particles depicted in Fig. 10.11 resulted in high white light photoactivated performance for degradation of rhodamine B (Zhuo et al. 2013). Spherical Bi_2WO_6 nanoparticles were fabricated via hydrothermal route with average size 85 nm bear great photoactivity for elimination of rhodamine B under solar light (Wang et al. 2015). Bi_2WO_6 with nanoplate two-dimensional structure with 30 nm length size exhibited high performance for photoactivated remediation of aquatic solution of rhodamine B under solar light which could be related to small particle size and high surface area (Zhang and Zhu 2005). Another work reported the hydrothermal preparation of nanoplate Bi_2WO_{6-x} with high surface oxygen vacancy with 2.1 times higher photocatalytic degradation of 2–4-dichlorophenol than pristine Bi_2WO_6 (Lv et al. 2016). High photocatalytic performance can attribute to high surface oxygen vacancy states.

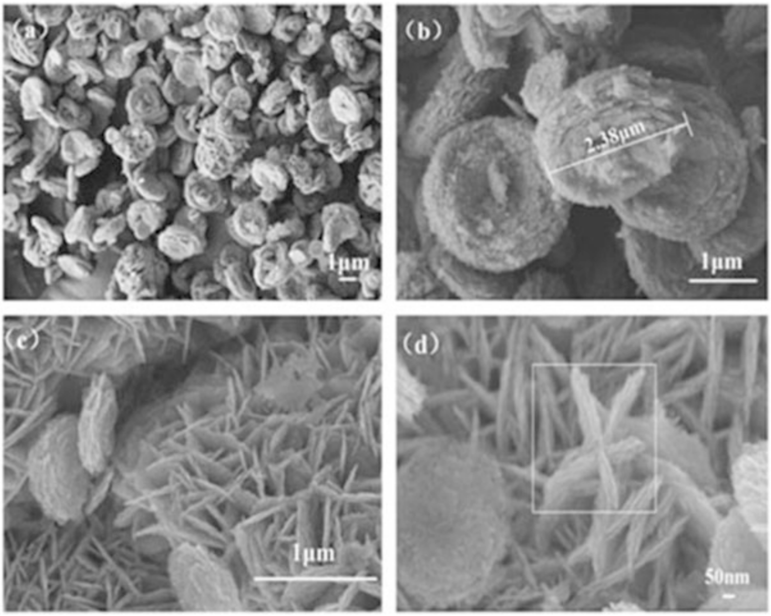

Fig. 10.11 Scanning electron microscopy images of Bi_2WO_6 with different morphologies synthesized at pH = 1 and pH = 5. (Reprinted with permission of Elsevier from Zhuo et al. 2013)

One-dimensional Bi_2MoO_6 nanosheets were fabricated via electrospinning which demonstrated remarkable photocatalytic efficiency within remediation of rhodamine B and methylene blue under simulated visible light (Sun et al. 2013b).

Hierarchical Bi−compounds

Hierarchical structures can be highlighted as ordered architectures assembled from low- dimensional building blocks, such as nanofibers, nanorods, nanoribbons, nanosheets, and nanoplates. Recently, great attention has been attracted to hierarchical assemblies due to the proper electronic, optical properties, layered structure, and catalytic efficiency which has bold difference with low-dimensional sub-component (Luo et al. 2019; Song et al. 2019). Herein, the synthesis of hierarchical Bi−compounds has attracted more efforts from the view of specific morphologies to gain high photocatalytic performance. The hierarchical Bi_2WO_6 hollow tubes demonstrated high photo-induced catalytic efficiency for elimination of rhodamine B under simulated visible light, which was related to Bi_2WO_6 structure, tight band gap, and gross surface area (Yafei et al. 2013). Zargazi et al. indicated the high simultaneous photocatalytic and sonophotocatalytic performances of Bi_2WO_6 nanoflowers for binary mixture (methylene blue and rhodamine B) synthesized by ultrasonic-assisted hydrothermal which attributed effect of morphology in

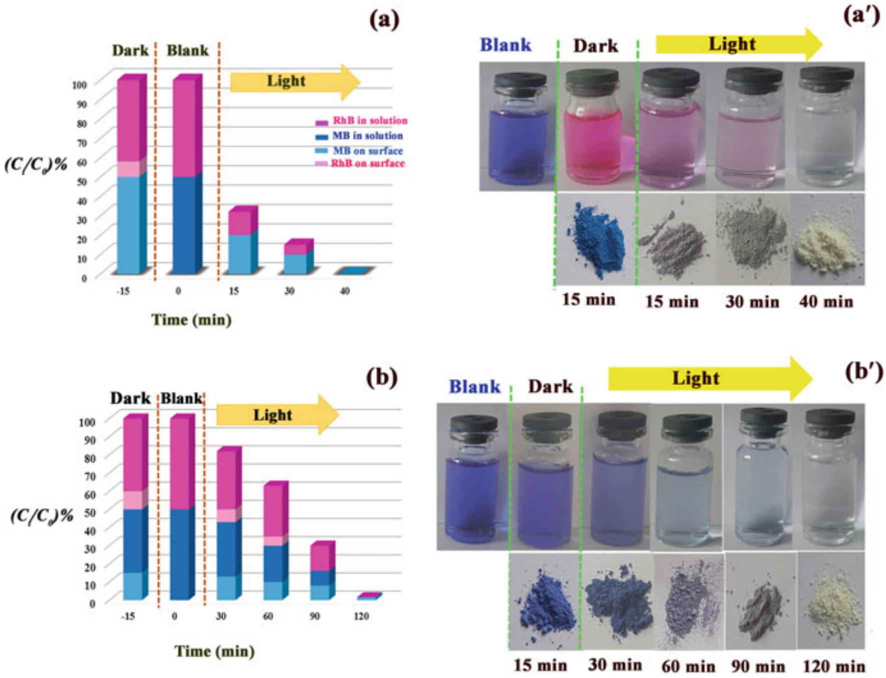

Fig. 10.12 Adsorption behaviors (dark) and sonophotocatalytic (light and US) degradation of rhodamine B/methylene B: Sono-BWO sample (a and a′), Hydro-BWO sample (b and b′). (Reprinted with permission of Elsevier from Zargazi and Entezari 2019c)

adsorption of pollutants from binary mixtures (Zargazi and Entezari 2019c). Both dyes were decomposed on the catalyst surface and bulk solution by sonophotocatalytic process which is observed in Fig. 10.12. Hierarchical flowerlike Bi_2MoO_6 crystals synthesized by simple hydrothermal method show permanent photo-induced reduction of CO_2 into methanol and ethanol (Dai et al. 2016). Morphology of Bi_2MoO_6 flower showed high influence in separation of photogenerated electron−hole and adsorption of light. Sharma et al. reported the preparation of Bi_2S_3 nanoflowers which exhibited the high photocatalytic degradation of two different binary mixtures of rhodamine B and methylene blue and 4-nitrophenol and 4-chlorophenol from suspension (Sharma and Khare 2018). Novel nanoflower structures of BiOCl with small band gap about 2.87 eV but huge average size about 1.5 μm were routinely prepared at 25 °C using the L−Lysine template. The interesting structure indicated high photocatalytic remediation of rhodamine B under solar light. The observed perfect photocatalytic performance can be appropriated to phase purity, high exposure of {110} planes, thin nano-petals structure, tight band gap, and the relatively large surface area.

Nano Bi Films

Recently, nano thin films of Bi−compounds attracted great attentions due to special applications in multiple fields such as water splitting, solar cell, and remediation environmental (Patil et al. 2015; Lee and Ebong 2017). Generally, powder compounds have serious problems including recollection and reusing, agglomeration effect, and respiration problems for human. To resolve problem's powders, immobilized films introduced as new solution for photocatalytic applications. Until now, Bi−films prepared by various methods such as chemical bath deposition (Gao et al. 2011), liquid phase deposition (Song et al. 2004), spin coating (Tyagi et al. 2015), sol−gel (Zargazi and Entezari 2019a), chemical vapor deposition (Brack et al. 2015), electrochemical deposition (Chahkandi and Zargazi 2019), electrophoretic deposition (Zargazi and Entezari 2019b), and so on.

Using the abovementioned methods, Bi−thin films deposited on conductive and non-conductive substrate were applied for degradation of various pollutants. For instance, Bi_2WO_6 deposited over the surface of stainless steel mesh using the anodic electrophoretic method and applied for remediation of binary mixture of 4−nitrophenol and 4−chlorophenol (Zargazi and Entezari 2019b). High photocatalytic degradation for film could be attributed to the effect of film thickness and substrate in separation of electron−hole. Alfaifi et al. reported the preparation of Bi_2WO_6 electrodes with nanoplates and Bucky ball-shaped microsphere morphologies by aerosol-assisted chemical vapor deposition which was applied for degradation of methylene blue and rhodamine B (Alfaifi and Bayahia 2019). Alfaifi and Bayahia suggested the energetic and interfacial features of Bi_2WO_6 film to increase solar energy and photocatalytic activity of film. $BiFeO_3$ film also deposited on the same substrate by anodic electrophoretic deposition method which exhibited high photocatalytic efficiency for decomposition of rhodamine B dye (Zargazi and Entezari 2018). $BiFeO_3$ film demonstrated higher photocatalytic degradation than $BiFeO_3$ powder due to substrate effect in decreasing of recombination rate of photo-induced charge pairs. At another work, forestlike $BiFeO_3$ films are fabricated by using cathodic electrophoretic deposition on the stainless steel mesh which indicated high photocatalytic performance for phenol compounds. Forestlike morphology of $BiFeO_3$ film depicts in Fig. 10.13 shows key effect in harvesting and multi-scattering of visible light which led to high degradation efficiency (Zargazi and Entezari 2019a). Venkatesan et al. (2018) shown the preparation of stable monoclinic − BiVO4 film by radio frequency − sputtering on the fluoride tin oxide and the degradation application of rhodamine 6G. Photocatalytic reduction of Cr hexavalent is conducted by Bi_2S_3 films in single and binary mixtures. Chahkandi et al. reported the novel deposition square wave voltammetry method of Bi_2S_3 film on the stainless steel mesh which exhibited high reduction rate for conversion toxic Cr(VI) to non-toxic Cr(III) (Chahkandi and Zargazi 2019).

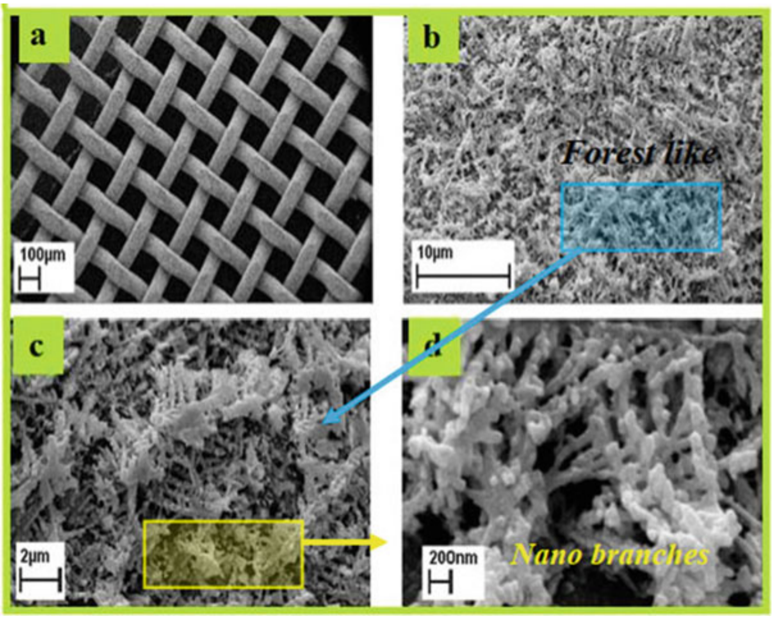

Fig. 10.13 $BiFO_3$ film coated on substrate (stainless steel mesh) (**a**), $BiFO_3$ film on wire surface (**b**), treelike structure (**c**) and nanobranches of $BiFO_3$ (**d**). (Reprinted with permission of Elsevier from Zargazi and Entezari 2019a)

Heterojunction

Over the past decades, designing of heterojunctions was introduced as a best route to reduce the recombination rate of electron−hole produced under light irradiation (Wang et al. 2014; Huang et al. 2015a). The Bi-based photocatalysts, with an appropriate band gap, have capability to produce electrons under solar light. However, the excited electron and holes potentially recombined very fast together. From this view, heterojunction construction can have a great role in enhancing photocatalytic efficiencies of Bi-based photocatalysts. Bi-based heterojunctions include conventional and Z−scheme heterojunctions. Among the conventional heterojunctions, the type II junction is the most usual one, while in Z−scheme type, the newly merged direct Z−scheme heterojunction appears to be the most effective junction structure used for exploring the capacity of photo-generated carriers (Wang et al. 2014; Low et al. 2017). Figure 10.14 depicted schematics for heterojunctions (Type II) and Z−scheme heterojunction.

Binary Bi are heterojunctions with two kinds of Bi−compounds, and also Binary Bi compounds can produce heterojunctions with non-Bi−compound.

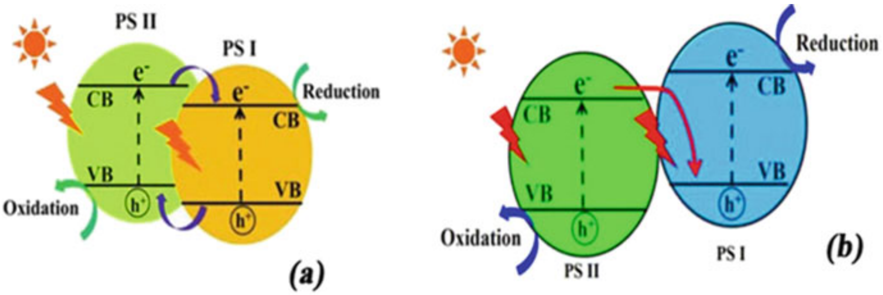

Fig. 10.14 Charge separation of (**a**) heterojunction (Type II) and (**b**) direct Z-scheme heterojunction. CB, VB, and PS stand for conductive band, valence band, and photocatalyst semiconductors, respectively. (Modified)

Type II: Conventional Heterojunction

In comparison with the trinary types of heterojunctions, the second junction type is the most suitable one. Bi-compounds and semiconductors with small band gap formed heterojunction (type II) as conduction band and valence band levels of semiconductors should be lower than the Bi−compound portion. For example, Fan et al. (2016) fabricated a binary Bi−compounds Bi_2MoO_6-BiOI heterojunction (Fig. 10.15a, b) by anion exchange method which exhibited high photocatalytic degradation efficiency for rhodamine B in comparison with BiOI or Bi_2MoO_6 alone (Fig. 10.15c). Optimal molar ratio of Mo/I is 50% made heterojunction (Type II) between two components having highest efficiency under white light (Fig. 10.15d). It is notable that three matched Bi−compounds can be combined together to produce a ternary heterojunction such as $Bi_2S_3/Bi_2O_3/MoS_2$ (Ke et al. 2017). Improved photocatalytic activity of $Bi_2S_3/Bi_2O_3/MoS_2$ ternary Bi−compounds can be attributed to enhancing of light adsorption and high separation of electron−hole by double heterojunction (Type II) (Fig. 10.16). Moreover, some other heterojunctions with low band gap semiconductors such as non-Bi−compounds were performed for improving photocatalytic degradation of different pollutants.

For instance, $g-C_3N_4$ compounds could be coupled with Bi_2WO_6, $BiVO_4$, Bi_2S_3, Bi_2O_3, and Bi_2MoO_6 which exhibited improved photocatalytic properties in degradation of pollutants. Numerous synthesis strategies for heterojunctions (Type II) have been introduced, and most of Bi-based heterojunctions led to improve photocatalytic efficiency (Table 10.1).

Direct Z-Scheme Heterojunctions

Yu et al. (2013) introduced a direct Z−scheme heterojunction to clarify the improvement of photocatalytic property of a $TiO_2/g-C_3N_4$ composite. The reported type of Z−scheme heterojunction does not need electron medium unlike other Z−scheme heterojunctions such as liquid phase. Built-in electric field between the interface of

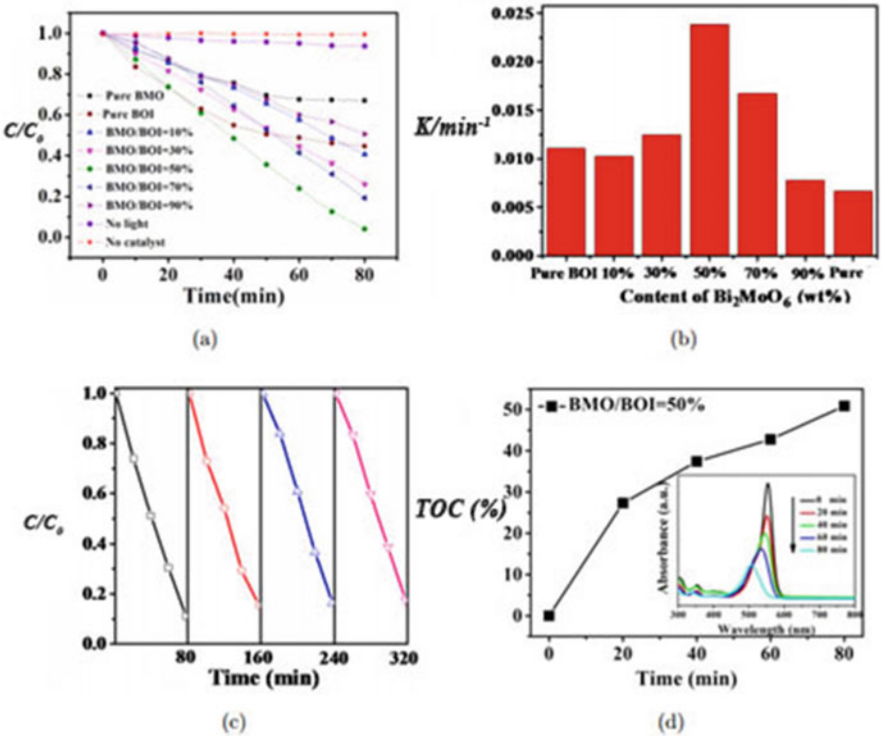

Fig. 10.15 (**a**) Photocatalytic degradation of rhodamine B. (**b**) The rate constants for Rhodamine B degradation on BOI, Bi_2MO_6, and Bi_2MO_6/BOI composites. (**c**) Recycling. (**d**) Total organic carbon changes for photocatalytic degradation of rhodamine B by using Bi_2MO_6/BOI = 50% as photocatalyst. (Reprinted with permission of World Scientific from Fan et al. 2016)

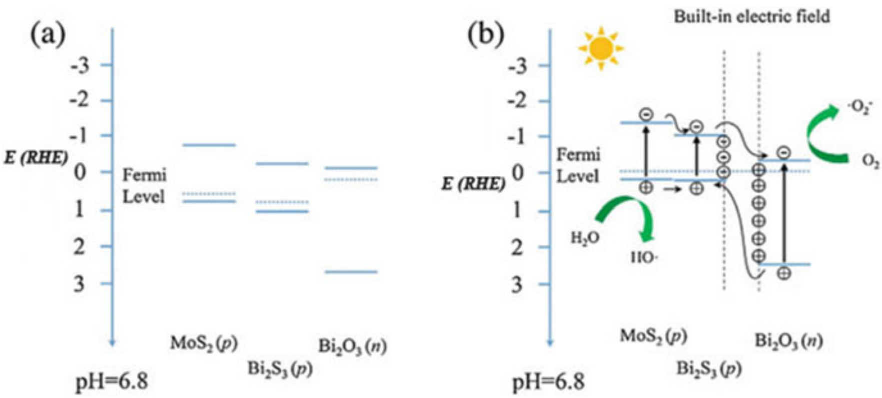

Fig. 10.16 Diagram for (**a**) energy band of Bi_2O_3, MoS_2, and Bi_2S_3 and (**b**) the formation of the three-phase p−n heterojunction and the possible charge separation. (Reprinted with permission of Elsevier from Ke et al. 2017)

Table 10.1 Some heterojunctions of Bi−based with Bi and non−Bi semiconductors

Bi-base	Second element	Method	Application	References
Bi-Binary heterojunctions				
Bi_2O_3	$BiVO_4$	Alkaline etching	RhB[a]	Han et al. (2013)
Bi_2S_3	Bi_2WO_6	Anion exchange	RhB	Yan et al. (2017)
Bi_2S_3	BiOCl	Solvothermal	SA[b]	Mi et al. (2017)
Bi_2MoO_6	BiOI	Ion exchange	RhB	Fan et al. (2016)
BiOI	$BiVO_4$	Precipitation	MO[c]	Ni et al. (2018)
BiOI	Bi_2MoO_6	Precipitation	BPA[d]	Yan et al. (2015)
BiOCl	$BiVO_4$	Co-precipitation	RhB	Gomez et al. (2018)
BiOCl	$Bi_{12}O_{17}C_{12}$	Hydrothermal	MO	Hao et al. (2017)
Non-Bi heterojunctions				
Bi_2O_3	$FeVO_4$	Calcination	Malachite green	Liu and Kang (2016)
Bi_2O_3	g-C_3N_4	Self-assembly	RhB	Dang et al. (2015)
Bi_2S_3	ZnS	Cation exchange	MB[e]	Xiong et al. (2011)
$BiFeO_3$	g-C_3N_4	Hydrothermal	Guaiacol	An et al. (2016)
$BiFeO_3$	CuO	Hydrothermal	MO	Niu et al. (2015)
$BiVO_4$	g-C_3N_4	Ultrasonic assembly	CO_2 reduction	Huang (2015)
$BiVO_4$	CeO_2	Co-precipitation	MB/MO	Wetchakun et al. (2012)
Bi_2WO_6	TiO_2	Hydrothermal	RhB, MO	Xu et al. (2018)
Bi_2MoO_6	g-C_3N_4	Solvothermal	Phenol	Li et al. (2014)
Bi_2MoO_6	AgBr	Precipitation	RhB	Jonjana et al. (2016)
BiOCl	g-C_3N_4	Solvothermal	RhB	Song et al. (2017)
BiOCl	CuS	Hydrothermal	RhB	Wang et al. (2015)
BiOI	TiO_2	Impregnation	MO	Wang et al. (2016)

[a]Rhodamine B, [b]Salicylic acid, [c]Methyl orange, [d]Bisphenol A, [e]Methyl orange

two semiconductors (I, II) acted as cite for charge transfer. The Z−scheme heterojunction has the same structure to a conventional heterojunction (type II), while charge transfer is different for two heterojunctions (Fig. 10.14b). In a Z−scheme heterojunction, charge transferring occurred by the built-in field at the interface of two semiconductors, while spatial separation conducted in heterojunction (type II). Cost-effective and high redox ability are the most prominent features for direct Z−scheme heterojunction. Numerous Bi-based Z−scheme heterojunctions have been fabricated and suggested. For example, BiOBr/g−C_3N_4 direct Z−scheme heterojunction was prepared via simple reflux method. The resulted BiOBr/g−C_3N_4 indicated more photocatalytic efficiency for remediation of rhodamine B, levofloxacin in comparison with BiOBr, or g−C_3N_4 alone. Meanwhile, $BiVO_4$ and Ag_3VO_4 composited together under hydrothermal treatment to form direct Z−scheme. The obtained composite has high photocatalytic activity for degradation and reduction of bisphenol and Cr(VI), respectively (Jing et al. 2019). Ternary Z−scheme heterojunctions synthesized for Bi-based compounds such as Bi_2WO_6/g−C_3N_4/rGO show enhanced efficiency by transferring of electrons

Table 10.2 Some of synthesized Z-scheme heterojunctions for Bi-based materials

Bi-Base	Other element	Method	Application	References
Double Z-scheme				
Bi_2O_3	g-C_3N_4	In situ calcination	MB	Liu et al. (2018)
Bi_2WO_6	MoS_2	Hydrothermal	RhB	Wang et al. (2017)
Bi_2MoO_6	BiOBr	Solvothermal	MB	Hu et al. (2018)
$BiVO_4$	Ag_3VO_4	Hydrothermal	Cr(VI), Bisphenol	Jing et al. (2019)
BiOI	g-C_3N_4	Hydrothermal/stirring	MB	Zhang et al. (2018)
BiOBr	g-C_3N_4	Reflux	RhB, levofloxacin	Shi et al. (2013)
BiOCl	g-C_3N_4	Chemical bath deposition	RhB	Bai et al. (2014)
Ternary Z-scheme				
Bi_2WO_6	g-C_3N_4/rGO	Hydrothermal	2,4,6Trichlorophenol	Ma et al. (2016)
Bi_2MoO_6	Ag/Ag_3PO_4	In situ-precipitation	RhB	Lin et al. (2015)
$BiVO_4$	$ZnIn_2S_4$/g-C_3N_4	Wet-impregnation	CR[a], MTN[b]	Zhu et al. (2019)
BiOI	UIO-66/g-C_3N_4	In situ, solvo-hydrothermal	RhB, TC[c]	Liang et al. (2018)
BiOCl	CQD-$SnNb_2O_6$	Hydrothermal	Benzocaine	Jiang et al. (2019)
BiOBr	r-GO/g-C_3N_4	Solvothermal	RhB, phenol	Bao and Chen (2018)

[a]Congo red, [b]Metronidazole, [c]Tetracycline

between double Z−scheme heterojunctions. Some of Z−scheme heterojunctions including Bi-compounds are summarized in Table 10.2.

10.3 Application

10.3.1 Water Remediation

According to previous section, the function of Bi-based photocatalysts through water remediation was extended. Bi-based nanocomposites, plasmonic composites, and carbon-based are the most famous composites which are applied for degradation of pollutants existed in water [134–167]. Existed pollutants include dyes, pharmaceutical, phenolic compounds, and toxic heavy metals. Table 10.3 shown some of Bi−compounds and composites in two forms of powder and film which applied for degradation of pollutants.

Table 10.3 Some of Bi−based photocatalyts in powder and film forms used for water remediation

Bi-based	Method	Performance	References
Bi-based powder			
Bi_2O_3	Solid-state	RhB	Oudghiri-Hassani et al. (2015)
Bi_2S_3	Hydrothermal	RhB, 1.5 h	Jia et al. (2016)
	Hot injection	RhB, 2 h	Wu et al. (2010)
	Hydrothermal	RhB/MB, 2 h	Sharma and Khare (2018)
$BiFeO_3$	Sonochemistry	MB	Soltani and Entezari (2013a, b, c)
	Sonochemistry	RhB	Soltani and Entezari (2013c)
	Hydrothermal	MO, 3 h	Niu et al. (2015)
Bi_2WO_6	Sonochemistry	MB/RhB	Zargazi and Entezari (2019c)
	CTAB-hydrothermal	RhB, 1 h	Yuxue Zhou (2017)
Bi_2MoO_6	Co-precipitation	MB, 6 h	Guo et al. (2018b)
	Solvothermal	RhB, 20 min	Li et al. (2013)
	Hydrothermal	RhB, 3 h	Phuruangrat et al. (2013)
$BiVO_4$	Microwave	MB, 5 h	Intaphong et al. (2016)
	Hydrothermal	RhB, 2 h	Ran et al. (2015)
	Solid phase	Cr, 30%, 2 h	Li et al. (2019)
	Thermal decomposition	MB, 105 min	Sivakumar et al. (2015)
BiOCl	Precipitation, calcination	RhB, 100 min	Xiong et al. (2011)
	Hydrolysis	MO, 9 h	Zhang et al. (2006)
BiOBr	Solvothermal	RhB, 2 h	Feng et al. (2015)
	Solvothermal	Acid Gallic	Mera et al. (2018)
BiOI	Soft chemical	MO, 3 h	Wang et al. (2011)
	Chemical bath deposition	RhB, Cr (VI)	Lv et al. (2018)
Bi-based film			
Bi_2O_3	Spray pyrolysis	MO, 3 h	Barrera-Mota et al. (2015)
	Sol-gel	RhB, 3.5 h	Weidong et al. (2007)
	EPD[a]	RB, 2 h	Guo et al. (2015)
Bi_2S_3	Hydrothermal	MB, 4 h	Tang et al. (2016)
	Electrodeposition	RhB/Cr, 1.5 h	Chahkandi and Zargazi (2019)
$BiFeO_3$	EPD	RhB	Zargazi and Entezari (2018)
	Sol-EPD	Phenol	Zargazi and Entezari (2019a)
Bi_2WO_6	EPD	4-NP[b]/4-CP[c]	Zargazi and Entezari (2019b)
	Spin coating	MB, 5 h	Zhang et al. (2009)
Bi_2MoO_6	Thermal evaporation	RhB, 10 h	Cuéllar et al. (2011)
	Reactive Magnetron deposition	RhB (80%), MB (60%), 1 h	Ratova et al. (2016)
	Dip-coating	. . .	Man (2007)

(continued)

Table 10.3 (continued)

Bi-based	Method	Performance	References
$BiVO_4$	Sputtering	Rh6G, 4 h	Venkatesan et al. (2018)
	Spray pyrolysis	RhB, 3 h	Ravidhas et al. (2018)
	Pulsed laser deposition	...	Jeong et al. (2016)
BiOCl	Dip-coating	RhB, 10 h	Liang et al. (2013)
	Sol-gel	RhB, 90 min	Wu et al. (2011)
	Alcoholysis-coating	MO, 150 min	Xiaoxia et al. (2012)
BiOI	Sol-gel	BPA, 2 h	Zhang et al. (2019)
	Dip-hydrothermal	RhB, 2 h	Wang et al. (2017)
BiOBr	Solvothermal	RhB, 3 h	Huo et al. (2015)
	Alcoholysis-coating	MO, 2.5 h	Li et al. (2014)

[a]Electrophoretic deposition, [b]4-Nitrophenol, [c]4-chlorophenol

10.3.2 Water Splitting

Energy frugality in the near future will be a major challenge around the world. Scientists are focused on researches providing clean and sustainable energy sources to decrease probability of complete disappear the unrenewable energies and to manage the pollutants. Burning of hydrogen in the presence of oxygen is not emitted any contaminants. Hence, hydrogen can be considered as a promising renewable fuel which is applied in vehicles, aircrafts, and electrical devices. Water splitting is a promising way to produce H_2. Different techniques for water splitting have been applied such as photoelectrochemical systems (Chen et al. 2016b), photocatalytic (Ni et al. 2007), photobiological (Poudyal et al. 2015), and thermal decomposition (Lapicque 1983). Among them, photoelectrochemical and photocatalytic water splitting are known as simplest, cost-effective, and efficient methods for hydrogen production which mechanism of H_2 production depicted in Fig. 10.17 (Abe 2011).

Photoelectrochemical water splitting manners are categorized in three types which are depicted in Fig. 10.18. The solar light is considered as effective source by Z−scheme compared to the conversional process. Therefore, the hydrogen evolution occurred under proton reduction by electrons of conduction band and oxygen evolution take place by holes of valence band. It can be concluded that the water hydrolysis progressed through the event of cyclic redox pair. Figure 10.18a, b shows n- and p-type semiconductors involved in water splitting. Figure 10.18c illustrates the combination of two various photo electrodes, as oxidation and reduction reactions can be simultaneously done and can more effectively employ solar energy. Over the surface of nanomaterials having high ratio of surface to volume, the charge carriers are generated because of the reduced size with high surface area, different shapes, and controlled morphology. Therefore, nanomaterials can be applied in water splitting process established at the nanomaterials surface. Many researches demonstrate the 50–90% increment in the efficiency of photoelectrochemical water splitting.

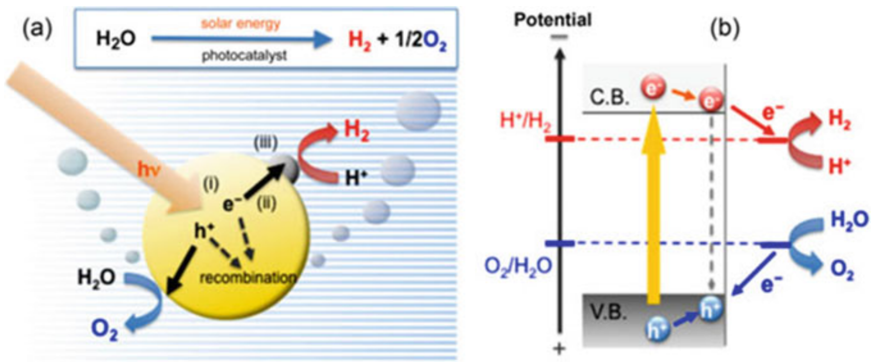

Fig. 10.17 (**a**) Mechanism of water splitting over semiconductor photocatalyst and (**b**) levels of conduction and valence bands for photocatalyst with overall water splitting efficiency. C.B. and V.B. stand for conductive band and valence band, respectively. (Reprinted with permission of Elsevier from Abe 2011)

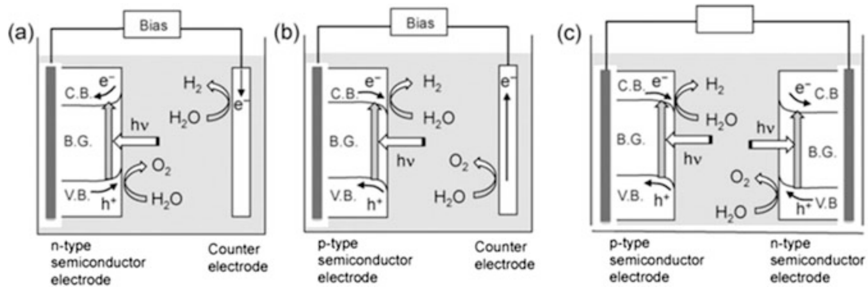

Fig. 10.18 Photoelectrochemical water splitting systems using n-type semiconductor (**a**), p-type semiconductor (**b**), and tandem system (**c**), C.B., V.B., and B.G. stand for conductive band, valence band, and band gap, respectively. (Reprinted with permission of Elsevier from Abe 2011)

The structural and electronic features of applied photo-anodes/cathodes in nanomaterials are the main factors affecting the photoelectrochemical water splitting mechanism. Various visible light materials were applied in photoelectrochemical water splitting as photo-electrodes. Recently, Bi-based materials have been widely used in the manufacturing of photo-electrodes in visible light materials systems. For instance, $BiFeO_3$ photo-anodes were synthesized by using dual-source low-pressure chemical vapor deposition and used in photocatalytic and photoelectrochemical water splitting induced by solar light. Results of incident photon-to-electron conversion efficiency suggested 23% efficiency for photoelectrochemical water splitting activated by light illumination (400 nm) (Moniz et al. 2015). Another work has reported high efficient nanoporous Bi_2WO_6 photo-anodes which synthesized by facile drop-casting method (Dong et al. 2017). The Bi_2WO_6 photo-electrode showed highly significant efficiency for photoelectrochemical water splitting which exhibited photocurrent almost ten times higher than traditional photo-electrodes.

Some of Bi-based compounds and nanocomposites synthesized by various methods and applied in photoelectrochemical and photocatalytic water splitting are reported in Table. 10.4.

10.4 Conclusions and Prospects

Some of special properties of Bi-based semiconductors, such as narrow band gap, layered structures, and controllable morphologies, have attracted more attentions from researchers in photocatalyst field. Almost all of Bi-based photocatalysts type and the catalytic applications have been discussed in this chapter. According to some challenges about Bi-based photocatalytic compounds, noted as fast recombination rate of electrons−hole and low light adsorption and practical approaches suggested to defeat the related challenges. Furthermore, main accomplished works until now have been summarized within morphology control and heterojunctions. However, probable problems for using Bi-based semiconductors can be disappeared, but further studies are still needed to improve the related progresses. Future works could be focused on below issues:

1. Until now, significant applications of Bi−nanomaterials can be highlighted as destruction of organic polluters and bacteria of wastewater and purification of air through denitration. Preparation of Z−scheme structures can be nominated as an applicable method for increasing the H_2 generation via photoactivated water splitting under solar light. Further works try to develop advanced Bi−nanomaterials to improve the applicable arena such as photocatalytic synthetization of organic compounds and photoactivated reduction for elimination of heavy metals.
2. Pragmatic applications of photocatalysts based on bismuth compounds are rarely storied. Designing the new applicable photocatalytic reactor can permanently precipitate the scale-up process. It can represent the potential industrialization capability of the advanced Bi−nanomaterial. Moreover, establishing of experiments by a solar simulator instead of a bulb shows the more reality of solar-activated photocatalysis performance of mentioned compounds.
3. The applicable fields along with further advancements can be propagated through consolidation of different useful techniques such as electrochemistry, membrane technique, and biotechnology. Despite many of bismuth-based semiconductors establish remarkable photoactivity efficiency induced by solar/visible light, they are far from full-fledged commercialization of the advanced nanomaterial. The perfect promised and interesting properties of Bi-based compounds can gift a bright future within environmental aspects and renewable energy sources.

Table 10.4 Some of Bi-compounds applied for water splitting

Bi-Based	Sort	Method	Performance	References
Bi_2WO_6	Electrode	Angle deposition	4.3 μA cm^{-2}	Larson and Zhao (2016)
N-Bi_2WO_6	Electrode	Drop-casting	120 μA cm^{-2} (1.23 V)	Dong et al. (2017)
P-Bi_2WO_6	Electrode	Drop casting	500 μA cm^{-2} (1V)	Dong et al. (2017)
Bi_2WO_6-Cu_3P	Suspension	Ball milling	9 μmolg^{-1} (H_2)	Rauf et al. (2018)
In_2O_3/Bi_2WO_6	Electrode	Chemical bath deposition	1.0 mA cm^{-2} (0.7 V)	Joshi (2015)
Bi_2MoO_6/TiO_2	Electrode	...	0.668 mmol$h^{-1}g^{-1}$ (O_2)	Wo et al. (2013)
$BiVO_4$	Electrode	Solvothermal	8 μA cm^{-2} (0.5 V)	Rani et al. (2019)
$BiVO_4$	Suspension	Solid-liquid state reaction	210 μmolh^{-1} (O_2)	Iwase et al. (2016)
Cu_2O/$BiVO_4$	Electrode	Electrodeposition	2.34 mA cm^{-2} (1.23 V)	Kim et al. (2018a)
TiO_2/$BiVO_4$	Electrode	Chemical bath deposition	0.8 mA cm^{-2} (1.23 V)	Cheng et al. (2016)
Co-Pi/$CuWO_4$/$BiVO_4$	Electrode	Drop casting	2.25 mA cm^{-2} (1.23 V)	Peng et al. (2018)
$ZnIn_2S_4$/RGO/$BiVO_4$	Suspension	Hydrothermal	180 μmolg^{-1} (H_2)	Zhu et al. (2019)
β-Bi_2O_3	Electrode	Spray deposition	0.97 mA cm^{-2} (0.5 V)	Kim et al. (2018b)
Pt–Bi_2O_3	Electrode	Aerosol-assisted chemical vapor deposition	3.1 μmol$g^{-1}h^{-1}$ (H_2)	Moniz et al. (2012)
Pt-Bi_2O_3/RuO_2	Suspension	Sonochemical hydrolysis	14.5 μmolg^{-1} h^{-1} (H_2)	Hsieh et al. (2013)
Bi_2O_3/WO_3	Electrode	Hydrothermal	0.85 μA cm^{-2}	Khan et al. (2016)
Bi_2O_3/Bi_2S_3/MoS_2	Electrode	Hydrothermal	529.1 μmol$h^{-1}g^{-1}$ (O_2)	Ke et al. (2017)
Bi_2O_3/$TiO_{2-x}N_x$	Suspension	Soft chemical rout	198.4 μmolh^{-1} (H_2)	Naik et al. (2011)
Bi_2O_3/Bi_2WO_6	Electrode	Pulse electrodeposition	35 μA cm^{-2}	Ying et al. (2018)
BiOCl	Suspension	Ionic liquid method	10.5 μA cm^{-2}	Stephenson et al. (2018)
BiOCl	Electrode	Chemical Vapor Deposition	...	Stephenson et al. (2018)
Bi-BiOCl	Electrode	In-situ photoelectroreduce	2.4 μmolh^{-1} (H_2)	Fan et al. (2017)

(continued)

Table 10.4 (continued)

Bi-Based	Sort	Method	Performance	References
BiOX ($X = Cl, Br, I$)	Electrode	Aerosol-assisted chemical vapour deposition	10.5 μA cm^{-2} (1.23 V)	Gomez et al. (2018)
Zn-BiOBr	Electrode	Doctor-blade	9.5 $\mu molh^{-1}$ (H_2)	Guo et al. (2018a)
Cu_2S-BiOBr	Suspension	Precipitation	717 $\mu molg^{-1}$ (H_2)	Paquin et al. (2015)
Bi_4NbO_8Cl	Suspension	Solid state reaction	30 $\mu molh^{-1}$ (O_2)	Fujito et al. (2016)

Acknowledgments MCH and MZ thankfully appreciate the financial support by the Hakim Sabzevari University and Ferdowsi University of Mashhad, Iran.

References

Abe R (2011) Recent progress on photocatalytic and photoelectrochemical water splitting under visible light irradiation. J Photochem Photobiol C Photochem Rev 11:179–209. https://doi.org/10.1016/j.jphotochemrev.2011.02.003

Ai Z, Ho W, Lee S (2011a) Efficient visible light photocatalytic removal of NO with BiOBr-graphene nanocomposites. J Phys Chem C 115:25330–25337. https://doi.org/10.1021/jp206808g

Ai Z, Huang Y, Lee S, Zhang L (2011b) Monoclinic α-Bi_2O_3 photocatalyst for efficient removal of gaseous NO and HCHO under visible light irradiation. J Alloys Compd 509:2044–2049. https://doi.org/10.1016/j.jallcom.2010.10.132

Akueus F (2012) Electrodeposited zno/zn photocatalysts for the degradation of benzene-toluene-xylene mixture in aqueous phase fotomangkin zno/zn electroendapan bagi degradasi campuran benzena-toluena-xilena. Malay J Anal Sci 16:277–282

Alahiane S, Qourzal S, Ouardi ME et al (2014) Factors influencing the photocatalytic degradation of reactive Yellow 145 by TiO_2-coated non-woven fibres. Am J Anal Chem 5:445–454. https://doi.org/10.4236/ajac.2014.58053

Alarfaj E (2016) Investigation of Ag-TiO_2 nanostructures photocatalytic properties prepared by modified dip coating method. Philos Mag 96:1386–1398. https://doi.org/10.1080/14786435.2016.1163432

Alfaifi BY, Bayahia H (2019) Highly efficient nanostructured Bi_2WO_6 thin film electrodes for photoelectrochemical and environment remediation. Nanomaterials 9:755

Aziz RA, Sopyan I (2010) Recent progress on development of TiO_2 thin film photocatalysts for pollutant removal. Recent Patents Mater Sci 2:88–111. https://doi.org/10.2174/1874465610902020088

Bai Y, Wang P-Q, Liu J-Y, Liu X-J (2014) Enhanced photocatalytic performance of direct Z-scheme BiOCl–g-C3N4 photocatalysts. RSC Adv 4(37):19456

Bao Y, Chen K (2018) Novel Z-scheme BiOBr/reduced graphene oxide/protonated g-C3N4 photocatalyst: synthesis, characterization, visible light photocatalytic activity and mechanism. Appl Surf Sci 437:51–61

Barrera-Mota K, Bizarro M, Castellino M et al (2015) Spray deposited β-Bi_2O_3 nanostructured films with visible photocatalytic activity for solar water treatment. Photochem Photobiol Sci 14:1110–1119. https://doi.org/10.1039/c4pp00367e

Brack P, Sagu JS, Peiris TAN et al (2015) Aerosol-assisted CVD of bismuth vanadate thin films and their photoelectrochemical properties. Chem Vap Depos 21:41–45. https://doi.org/10.1002/cvde.201407142

Buscaglia MT, Sennour M, Buscaglia V et al (2011) Formation of $Bi_4Ti_3O_{12}$ one-dimensional structures by solid-state reactive diffusion. From core-shell templates to nanorods and nanotubes. Cryst Growth Des 11:1394–1401. https://doi.org/10.1021/cg101697r

Chahkandi M, Zargazi M (2019) Novel method of square wave voltammetry for deposition of Bi_2S_3 thin film: photocatalytic reduction of hexavalent Cr in single and binary mixtures. J Hazard Mater 380:120879. https://doi.org/10.1016/j.jhazmat.2019.120879

Chen Z, Qian L, Zhu J et al (2010) Controlled synthesis of hierarchical Bi_2WO_6 microspheres with improved visible-light-driven photocatalytic activity. CrystEngComm 12:2100. https://doi.org/10.1039/b921228k

Chen L, He J, Liu Y et al (2016a) Recent advances in bismuth – containing photocatalysts with heterojunctions. Chin J Catal 37:780–791. https://doi.org/10.1016/S1872-2067(15)61061-0

Chen X, Zhang Z, Chi L, Nair AK (2016b) Recent advances in visible-light-driven photoelectrochemical water splitting: catalyst nanostructures and reaction systems. Nano-Micro Lett 8:1–12. https://doi.org/10.1007/s40820-015-0063-3

Cheng BY, Yang JS, Cho HW, Wu JJ (2016) Fabrication of an efficient $BiVO_4$-TiO_2 heterojunction photoanode for photoelectrochemical water oxidation. ACS Appl Mater Interfaces 8:20032–20039. https://doi.org/10.1021/acsami.6b05489

Cuéllar EL, Martínez-De La Cruz A, Rodríguez KHL, Méndez UO (2011) Preparation of γ-Bi_2MoO_6 thin films by thermal evaporation deposition and characterization for photocatalytic applications. Catal Today, In, pp 140–145

Dai W, Yu J, Xu H et al (2016) Synthesis of hierarchical flower-like Bi_2MoO_6 microspheres as efficient photocatalyst for photoreduction of CO_2 into solar fuels under. CrystEngComm. https://doi.org/10.1039/C6CE00248J

Dang X, Zhang X, Chen Y, Dong X, Wang G, Ma C, Zhang X, Ma H, Xue M (2015) Preparation of β-Bi2O3/g-C3N4nanosheet p–n junction for enhanced photocatalytic ability under visible light illumination. J Nanopart Res 17(2)

Dong G, Zhang Y, Wang W et al (2017) Facile fabrication of nanoporous Bi_2WO_6 photoanodes for efficient solar water splitting. Energ Technol 5:1912–1918. https://doi.org/10.1002/ente.201700138

Fan L, Wei B, Xu L et al (2016) Ion exchange synthesis of Bi_2MoO_6/BiOI heterojunctions for photocatalytic degradation and photoelectrochemical water splitting. Nano 11:1–10. https://doi.org/10.1142/S1793292016500958

Fan W, Li C, Bai H et al (2017) An in situ photoelectroreduction approach to fabricate Bi/BiOCl heterostructure photocathodes: understanding the role of Bi metal for solar water splitting. J Mater Chem A 5:4894–4903. https://doi.org/10.1039/c6ta11059b

Feng H, Wang L, Mitchell DRG (2015) Modulation of photocatalytic properties by strain in 2d BiOBr nanosheets. ACS Appl Mater Interfaces 7:27592–27596

Fujito H, Kunioku H, Kato D et al (2016) Layered perovskite oxychloride Bi_4NbO_8Cl: a stable visible light responsive photocatalyst for water splitting. J Am Chem Soc 138(7):2082–2085

Gao C, Shen H, Sun L, Shen Z (2011) Chemical bath deposition of Bi_2S_3films by a novel deposition system. Appl Surf Sci 257:7529–7533. https://doi.org/10.1016/j.apsusc.2011.03.080

Gao T, Chen Z, Huang Q et al (2015) A review: preparation of bismuth ferrite nanoparticles and its applications in visible-light induced photocatalyses. Rev Adv Mater Sci 40:97–109

Ge J, Zhang Y, Heo YJ, Park SJ (2019) Advanced design and synthesis of composite photocatalysts for the remediation of wastewater: a review. Catalysts 9(2):122

Gomez IJ, Arnaiz B, Cacioppo M et al (2018) Nitrogen-doped carbon nanodots for bioimaging and delivery of paclitaxel. J Mater Chem B 6:1–10. https://doi.org/10.1039/x0xx00000x

Guo W, Zhang S, Guo Y et al (2013) Template-free and morphology-controlled hydrothermal growth of single-crystalline $Bi_{12}TiO_{20}$ with excellent simulated sunlight photocatalytic activity. RSC Adv 3:4008–4017. https://doi.org/10.1039/c3ra22592e

Guo X, Li X, Lai C et al (2015) Cathodic electrophoretic deposition of bismuth oxide (Bi_2O_3) coatings and their photocatalytic activities. Appl Surf Sci 331:455–462. https://doi.org/10.1016/j.apsusc.2015.01.034

Guo AJ, Liao X, Lee M, Hyett G (2018a) Experimental and DFT insights of the Zn-doping effects on the visible-light photocatalytic water splitting and dye decomposition over Zn-doped BiOBr photocatalyst. Appl Catal B Environ. https://doi.org/10.1016/j.apcatb.2018.09.089

Guo J, Shi L, Zhao J et al (2018b) Enhanced visible-light photocatalytic activity of Bi_2MoO_6 nanoplates with heterogeneous Bi_2MoO_{6-x} @ Bi_2MoO_6 core-shell structure. Appl Catal B Environ 224:692–704. https://doi.org/10.1016/j.apcatb.2017.11.030

Han M, Sun T, Tan PY, Chen X, Tan OK, Tse MS (2013) M-BiVO4@γ-Bi2O3 core–shell p–n heterogeneous nanostructure for enhanced visible-light photocatalytic performance. RSC Adv 3(47):24964

Hao L, Huang H, Guo Y, Du X, Zhang Y (2017) Bismuth oxychloride homogeneous phasejunction BiOCl/Bi 12 O 17 Cl 2 with unselectively efficient photocatalytic activity and mechanism insight. Appl Surf Sci 420:303–312

He R, Xu D, Cheng B et al (2018) Review on nanoscale Bi-based photocatalysts. Nanoscale Horiz 3:464–504

Hou J, Qu Y, Krsmanovic D et al (2009) Solution-phase synthesis of single-crystalline $Bi_{12}TiO_{20}$ nanowires with photocatalytic properties. Chem Commun:3937–3939. https://doi.org/10.1039/b906290d

Hsieh SH, Lee GJ, Davies SH et al (2013) Synthesis of Cr_2O_3 and Pt doped RuO_2/Bi_2O_3 photocatalysts for hydrogen production from water splitting. Am J Environ Eng 3:115–120. https://doi.org/10.5923/j.ajee.20130303.01

Hu T, Yang Y, Dai K, Zhang J, Liang C (2018) A novel Z-scheme Bi2MoO6/BiOBr photocatalyst for enhanced photocatalytic activity under visible light irradiation. Appl Surf Sci 456:473–481

Huang WL, Zhu Q (2008) Electronic structures of relaxed BiOX (X = F, Cl, Br, I) photocatalysts. Comput Mater Sci 43:1101–1108. https://doi.org/10.1016/j.commatsci.2008.03.005

Huang Yan, Fu Min, He Tao (2015) 31 (6):1145-1152

Huang H, Han X, Li X et al (2015a) Fabrication of multiple heterojunctions with tunable visible-light-active photocatalytic reactivity in BiOBr-BiOI full-range composites based on microstructure modulation and band structures. ACS Appl Mater Interfaces 7:482–492. https://doi.org/10.1021/am5065409

Huang H, Li X, Wang J et al (2015b) Anionic group self-doping as a promising strategy: band-gap engineering and multi-functional applications of high-performance CO_{32}-doped $Bi_2O_2CO_3$. ACS Catal 5:4094–4103. https://doi.org/10.1021/acscatal.5b00444

Huang CK, Wu T, Huang CW et al (2017) Enhanced photocatalytic performance of $BiVO_4$ in aqueous $AgNO_3$ solution under visible light irradiation. Appl Surf Sci 399:10–19. https://doi.org/10.1016/j.apsusc.2016.12.038

Huang Y, Lin Y, Tong Y (2018) Ultrathin Bi_2MoO_6 nanosheets for photocatalysis: performance enhancement by atomic interfacial engineering. Energy Technol Environ Sci 3:1–7. https://doi.org/10.1002/slct.201800908

Huo Y, Hou R, Chen X et al (2015) BiOBr visible-light photocatalytic films in a rotating disk reactor for the degradation of organics. J Mater Chem A 3:14801–14808. https://doi.org/10.1039/c5ta03279b

Intaphong P, Phuruangrat A, Pookmanee P (2016) Synthesis and characterization of $BiVO_4$ photocatalyst by microwave method. Integr Ferroelectr 175:51–58. https://doi.org/10.1080/10584587.2016.1200910

Iwase A, Kato H, Kudo A (2016) A simple preparation method of visible-light-driven BiVO4 starting materials Bi2O3 and photocatalysts from oxide activities. J Sol Energy Eng 132:1–5. https://doi.org/10.1115/1.4001172

Jeevanandam J, Barhoum A, Chan YS et al (2018) Review on nanoparticles and nanostructured materials: history, sources, toxicity and regulations. Beilstein J Nanotechnol 9:1050–1074. https://doi.org/10.3762/bjnano.9.98

Jeong SY, Choi KS, Shin H et al (2016) Enhanced photocatalytic performance depending on morphology of bismuth vanadate thin film synthesized by pulsed laser deposition. ACS Appl Mater Interfaces. https://doi.org/10.1021/acsami.6b15034

Jia T, Wang X, Long F et al (2016) Facile synthesis, characterization, and visible-light photocatalytic activities of 3D hierarchical Bi_2S_3 architectures assembled by nanoplatelets. Crystals:6. https://doi.org/10.3390/cryst6110140

Jiang R, Lu G, Yan Z, Wu D, Zhou R, Bao X (2019) Insights into a CQD-SnNb2O6/BiOCl Z-scheme system for the degradation of benzocaine: influence factors, intermediate toxicity and photocatalytic mechanism. Chem Eng J 374:79–90

Jin J, He T (2017) Facile synthesis of Bi_2S_3nanoribbons for photocatalytic reduction of CO_2 into CH_3OH. Appl Surf Sci 394:364–370. https://doi.org/10.1016/j.apsusc.2016.10.118

Jing L, Lili Z, Benlin D, Jiming X (2019) A novel Z-scheme $Ag_3VO_4/BiVO_4$ heterojunction photocatalyst: study on the excellent photocatalytic performance and photocatalytic mechanism. Appl Catal B Environ. https://doi.org/10.1016/j.apcatb.2019.01.001

Jonjana S, Phuruangrat A, Thongtem T, Thongtem S (2016) Synthesis, analysis and photocatalysis of AgBr/Bi2MoO6 nanocomposites. Mater Lett 172:11–14

Joshi B (2015) Heterojunction photoanodes for solar water splitting using chemical-bath-deposited In_2O_3 micro-cubes and electro-sprayed Bi_2WO_6 textured nanopillars. RSC Adv 5:85323–85328. https://doi.org/10.1039/C5RA16833C

Ke J, Liu J, Sun H et al (2017) Facile assembly of $Bi_2O_3/Bi_2S_3/MoS_2$ n-p heterojunction with layered n -Bi_2O_3 and p -MoS_2 for enhanced photocatalytic water oxidation and pollutant degradation. Appl Catal B Environ 200:47–55. https://doi.org/10.1016/j.apcatb.2016.06.071

Khan I, Abdalla A, Qurashi A (2016) Synthesis of hierarchical WO_3 and Bi_2O_3/WO_3 nanocomposite for solar-driven water splitting applications. Int J Hydrog Energy:1–9. https://doi.org/10.1016/j.ijhydene.2016.11.105

Kim H, Bae S, Jeon D, Ryu J (2018a) Fully solution-processable Cu_2O-$BiVO_4$ photoelectrochemical cells for bias-free solar water splitting. Green Chem 20:3732–3742. https://doi.org/10.1039/c8gc00681d

Kim M, Joshi B, Samuel E et al (2018b) Highly nanotextured b -Bi_2O_3 pillars by electrostatic spray deposition as photoanodes for solar water splitting. J Alloys Compd 764:881–889. https://doi.org/10.1016/j.jallcom.2018.06.047

Kudo A, Omori K, Kato H (1999) A novel aqueous process for preparation of crystal form-controlled and highly crystalline $BiVO_4$ powder from layered vanadates at room temperature and its photocatalytic and photophysical properties. J Am Chem Soc 121:11459–11467. https://doi.org/10.1021/ja992541y

Kumar A (2017) A review on the factors affecting the photocatalytic degradation of hazardous materials. Mater Sci Eng Int J 1:1–10. https://doi.org/10.15406/mseij.2017.01.00018

Lam SM, Sin JC, Mohamed AR (2017) A newly emerging visible light-responsive $BiFeO_3$ perovskite for photocatalytic applications: a mini review. Mater Res Bull 90:15–30

Lapicque F (1983) Production of hydrogen by direct thermal decomposition of water. Int J Hydrog Energy 8:675–679

Larson S, Zhao Y (2016) Tuning the composition of Bi_xW_yO nanorods towards zero bias PEC water splitting. Nanotechnology 27:1–12. https://doi.org/10.1088/0957-4484/27/25/255401

Lee TD, Ebong AU (2017) A review of thin film solar cell technologies and challenges. Renew Sust Energ Rev 70:1286–1297. https://doi.org/10.1016/j.rser.2016.12.028

Lei Y, Wang G, Song S et al (2009) Synthesis, characterization and assembly of BiOCl nanostructure and their photocatalytic properties. CrystEngComm 11:1857–1862. https://doi.org/10.1039/b909013b

Li G, Ding Y, Zhang Y et al (2011) Microwave synthesis of BiPO4 nanostructures and their morphology-dependent photocatalytic performances. J Colloid Interface Sci 363:497–503. https://doi.org/10.1016/j.jcis.2011.07.090

Li Z, Chen X, Xue Z (2013) Bi_2MoO_6 microstructures: controllable synthesis, growth mechanism, and visible-light-driven photocatalytic activities. CrystEngComm 15:498–508. https://doi.org/10.1039/c2ce26260f

Li R, Fan C, Zhang X et al (2014) Preparation of BiOBr thin films with micro-nano-structure and their photocatalytic applications. Thin Solid Films. https://doi.org/10.1016/j.tsf.2014.04.077

Li L, Ma Z, Bi F et al (2016) Sol-gel preparation and properties of $Bi_4Ti_3O_{12}$ photocatalyst supported on micrometer-sized quartz spheres. J Adv Oxid Technol 19:310–316. https://doi.org/10.1515/jaots-2016-0215

Li X, Xie J, Jiang C et al (2018) Review on design and evaluation of environmental photocatalysts. Front Environ Sci Eng 12:1–32

Li J, Chen Y, Chen C, Wang S (2019) Solid-phase synthesis of visible-light-driven $BiVO_4$ photocatalyst and photocatalytic reduction of aqueous Cr (VI). Bull Chem React Eng Catal 14:336–344. https://doi.org/10.9767/bcrec.14.2.3182.336-344

Liang Y, Guo C, Cao S et al (2013) A high quality BiOCl film with petal-like hierarchical structures and its visible-light photocatalytic property. J Nanosci Nanotechnol 13:919–923. https://doi.org/10.1166/jnn.2013.5972

Liang Q, Cui S, Jin J, Liu C, Xu S, Yao C, Li Z (2018) Fabrication of BiOI@UIO-66(NH2)@g-C3N4 ternary Z-scheme heterojunction with enhanced visible-light photocatalytic activity. Appl Surf Sci 456:899–907

Lin X, Hou J, Jiang S, Lin Z, Wang M, Che G (2015) A Z-scheme visible-light-driven Ag/Ag PO/Bi MoO photocatalyst: synthesis and enhanced photocatalytic activity. RSC Adv 5(127):104815–104821

Liu X, Kang Y (2016) Synthesis and high visible-light activity of novel Bi 2 O 3/FeVO 4 heterojunction photocatalyst. Mater Lett 164:229–231

Liu S, Chen J, Xu D, Zhang X, Shen M (2018) Enhanced photocatalytic activity of direct -scheme Bi O/g-C N composites via facile one-step fabrication. J Mater Res 33(10):1391–1400

Low J, Yu J, Jaroniec M et al (2017) Heterojunction photocatalysts. Adv Mater 29:1–20. https://doi.org/10.1002/adma.201601694

Luo B, Kim A, Smith JW et al (2019) Hierarchical self-assembly of 3D lattices from polydisperse anisometric colloids. Nat Commun:1–9. https://doi.org/10.1038/s41467-019-09787-6

Lv Y, Yao W, Zong R, Zhu Y (2016) Fabrication of wide-range-visible photocatalyst Bi_2WO_{6-x} nanoplates via surface oxygen vacancies. Sci Rep 6:1–9. https://doi.org/10.1038/srep19347

Lv Y, Li P, Che Y et al (2018) Facile Preparation and Characterization of Nanostructured BiOI microspheres with certain adsorption-photocatalytic properties. Mater Res 21

Ma D, Wu J, Gao M, Xin Y, Ma T, Sun Y (2016) Fabrication of Z-scheme g -C 3 N 4/RGO/Bi 2 WO 6 photocatalyst with enhanced visible-light photocatalytic activity. Chem Eng J 290:136–146

Mahlambi MM, Ngila CJ, Mamba BB (2015) Recent developments in environmental photocatalytic degradation of organic pollutants: the case of titanium dioxide nanoparticles – a review. J Nanomater 2015:1–29. https://doi.org/10.1155/2015/790173

Man Y (2007) Preparation and photoelectrochemical properties of Bi_2MoO_6 films. Acta Physico-Chimica Sinica 23:1671–1676

Meng X, Zhang Z (2016) Bismuth-based photocatalytic semiconductors: introduction, challenges and possible approaches. J Mol Catal A Chem 423:533–549

Mera AC, Rodríguez CA, Valdés H et al (2018) Solvothermal synthesis and photocatalytic activity of BiOBr microspheres with hierarchical morphologies. Acta Chimica Slovenica 65:429–437. https://doi.org/10.17344/acsi.2018.4181

Mi Y, Li H, Zhang Y, Zhang R, Hou W (2017) One-pot synthesis of belt-like Bi2S3/BiOCl hierarchical composites with enhanced visible light photocatalytic activity. Appl Surf Sci 423:1062–1071

Moniz SJA, Bhachu D, Blackman CS et al (2012) A novel route to Pt – Bi_2 O_3 composite thin films and their application in photo-reduction of water. Inorganica Chim Acta 380:328–335. https://doi.org/10.1016/j.ica.2011.09.029

Moniz SJA, Blackman CS, Southern P et al (2015) Visible-light driven water splitting over $BiFeO_3$ photoanodes grown via the LPCVD reaction of $[Bi(OtBu)_3]$ and $[Fe(OtBu)_3]_2$ and enhanced with a surface nickel oxygen evolution catalyst. Nanoscale 7:16343–16353. https://doi.org/10.1039/c5nr04804d

Myung N, Lee W, Lee C et al (2014) Synthesis of Au-$BiVO_4$ nanocomposite through anodic electrodeposition followed by galvanic replacement and its application to the photocatalytic decomposition of methyl orange. ChemPhysChem 15:2052–2057. https://doi.org/10.1002/cphc.201402032

Naik B, Martha S, Parida KM (2011) Facile fabrication of $Bi_2O_3/TiO_{2-x}N_x$ nanocomposites for excellent visible light driven photocatalytic hydrogen evolution. Int J Hydrog Energy 36:2794–2802. https://doi.org/10.1016/j.ijhydene.2010.11.104

Ni M, Leung MKH, Leung DYC, Sumathy K (2007) A review and recent developments in photocatalytic water-splitting using TiO2for hydrogen production. Renew Sust Energ Rev 11:401–425. https://doi.org/10.1016/j.rser.2005.01.009

Ni S, Zhou T, Zhang H, Cao Y, Yang P (2018) BiOI/BiVO two-dimensional Heteronanostructures for visible-light photocatalytic degradation of rhodamine B. ACS Applied Nano Materials 1(9):5128–5141

Niu F, Chen Z, Qin L (2015) Hydrothermal synthesis of $BiFeO_3$ nanoparticles for visible light photocatalytic applications. J Nanosci Nanotechnol 15(12):9693–9698. https://doi.org/10.1166/jnn.2015.10682

Opoku F, Govender KK, van Sittert CGCE, Govender PP (2017) Recent progress in the development of semiconductor-based photocatalyst materials for applications in photocatalytic water splitting and degradation of pollutants. Adv Sustain Syst 1:1700006. https://doi.org/10.1002/adsu.201700006

Oudghiri-Hassani H, Rakass S, Al Wadaani FT et al (2015) Synthesis, characterization and photocatalytic activity of α-Bi_2O_3 nanoparticles. J Taibah Univ Sci 9:508–512. https://doi.org/10.1016/j.jtusci.2015.01.009

Paquin F, Rivnay J, Salleo A et al (2015) Multi-phase semicrystalline microstructures drive exciton dissociation in neat plastic semiconductors. J Mater Chem C 3:10715–10722. https://doi.org/10.1039/b000000x

Patil M, Shaikh S, Ganesh I (2015) Recent advances on TiO_2 thin film based photocatalytic applications – a review. Curr Nanosci 11:271–285. https://doi.org/10.2174/1573413711666150212235054

Peng B, Xia M, Li C et al (2018) Network structured $CuWO_4/BiVO_4$/Co-Pi nanocomposite for solar water splitting ben. Catalysts:1–9. https://doi.org/10.3390/catal8120663

Phuruangrat A, Jitrou P, Dumrongrojthanath P et al (2013) Hydrothermal synthesis and characterization of Bi_2MoO_6 nanoplates and their photocatalytic activities. J Nanomater 2013. https://doi.org/10.1155/2013/789705

Ponraj C, Vinitha G, Daniel J (2017) A review on the visible light active $BiFeO_3$ nanostructures as suitable photocatalyst in the degradation of different textile dyes. Environ Nanotechnol Monit Manag 7:110–120

Poudyal RS, Koirala AR, Masukawa H, Inoue K (2015) Hydrogen production using photobiological methods. Compend Hydrog Energy:289–317. https://doi.org/10.1016/B978-1-78242-361-4.00010-8

Qin F, Li G, Wang R et al (2012) Template-free fabrication of Bi_2O_3 and $(BiO)_2CO_3$ nanotubes and their application in water treatment. Chem A Eur J 18:16491–16497. https://doi.org/10.1002/chem.201201989

Ran R, McEvoy JG, Zhang Z (2015) Synthesis and optimization of visible light active $BiVO_4$ photocatalysts for the degradation of RhB. Int J Photoenergy 2015. https://doi.org/10.1155/2015/612857

Rani BJ, Praveenkumar M, Ravichandran S et al (2019) $BiVO_4$ nanostructures for photoelectrochemical (PEC) solar water splitting applications. J Nanosci Nanotechnol 19:7427–7435. https://doi.org/10.1166/jnn.2019.16642
Ratova M, Kelly P, West G et al (2016) Deposition of visible light active photocatalytic bismuth molybdate thin films by reactive magnetron sputtering. Materials (Basel) 9:67–80. https://doi.org/10.3390/ma9020067
Rauf A, Ma M, Kim S et al (2018) Mediator- and co-catalyst-free direct Z-scheme composites of Bi_2WO_6-Cu_3P for solar-water splitting. Nanoscale 10:3026–3036. https://doi.org/10.1039/c7nr07952d
Ravidhas C, Arivukarasan D, Venkatesh R et al (2018) Substrate temperature induced (040) growth facets of nebulizer sprayed $BiVO_4$ thin films for effective photodegradation of rhodamine B. 1700257:1–11. https://doi.org/10.1002/crat.201700257
Reddy CV, Babu B, Reddy IN, Shim J (2018) Synthesis and characterization of pure tetragonal ZrO_2 nanoparticles with enhanced photocatalytic activity. Ceram Int 44:6940–6948. https://doi.org/10.1016/j.ceramint.2018.01.123
Schwarzenbach RP, Egli T, Hofstetter TB et al (2010) Global water pollution and human health. Annu Rev Environ Resour 35:109–136. https://doi.org/10.1146/annurev-environ-100809-125342
Shang M, Wang W, Zhang L (2009) Preparation of BiOBr lamellar structure with high photocatalytic activity by CTAB as Br source and template. J Hazard Mater 167:803–809. https://doi.org/10.1016/j.jhazmat.2009.01.053
Sharma S, Khare N (2018) Hierarchical Bi_2S_3 nanoflowers: a novel photocatalyst for enhanced photocatalytic degradation of binary mixture of rhodamine B and methylene blue dyes and degradation of mixture of p-nitrophenol and p-chlorophenol. Adv Powder Technol 29:3336–3347. https://doi.org/10.1016/j.apt.2018.09.012
Shi X, Chen X, Chen X et al (2013) PVP assisted hydrothermal synthesis of BiOBr hierarchical nanostructures and high photocatalytic capacity. Chem Eng J 222:120–127. https://doi.org/10.1016/j.cej.2013.02.034
Shimodaira Y, Kato H, Kobayashi H, Kudo A (2006) Photophysical properties and pbotocatalytic activities of bismuth molybdates under visible light irradiation. J Phys Chem B 110:17790–17797. https://doi.org/10.1021/jp0622482
Sivakumar V, Suresh R, Giribabu K (2015) $BiVO_4$ nanoparticles: preparation, characterization and photocatalytic activity. Cogent Chem 133:1–10. https://doi.org/10.1080/23312009.2015.1074647
Soltani T, Entezari MH (2013a) Solar photocatalytic degradation of RB5 by ferrite bismuth nanoparticles synthesized via ultrasound. Ultrason Sonochem 20:1245–1253. https://doi.org/10.1016/j.ultsonch.2013.01.012
Soltani T, Entezari MH (2013b) Sono-synthesis of bismuth ferrite nanoparticles with high photocatalytic activity in degradation of Rhodamine B under solar light irradiation. Chem Eng J 223:145–154. https://doi.org/10.1016/j.cej.2013.02.124
Soltani T, Entezari MH (2013c) Photolysis and photocatalysis of methylene blue by ferrite bismuth nanoparticles under sunlight irradiation. J Mol Catal A Chem 377:197–203. https://doi.org/10.1016/j.molcata.2013.05.004
Song DW, Shen W-N, Dunn B et al (2004) Thermal conductivity of nanoporous bismuth thin films. Appl Phys Lett 84:1883–1885. https://doi.org/10.1063/1.1682679
Song L, Pang Y, Zheng Y, Ge L (2017) Hydrothermal synthesis of novel g-C3N4/BiOCl heterostructure nanodiscs for efficient visible light photodegradation of rhodamine B. Applied Physics A 123(8)
Song G, Li J, Yuan Y et al (2019) Large-area 3D hierarchical superstructures assembled from colloidal nanoparticles. Small 15:1–8. https://doi.org/10.1002/smll.201805308
Stephenson J, Celorrio V, Tiwari D et al (2018) Photoelectrochemical properties of BiOCl microplatelets. J Electroanal Chem 819:171–177. https://doi.org/10.1016/j.jelechem.2017.10.024

Su W, Wang J, Huang Y et al (2010) Synthesis and catalytic performances of a novel photocatalyst BiOF. Scr Mater 62:345–348. https://doi.org/10.1016/j.scriptamat.2009.10.039

Sun Y, Cheng H, Gao S et al (2012) Atomically thick bismuth selenide freestanding single layers achieving enhanced thermoelectric energy harvesting. J Am Chem Soc 134:20294–20297. https://doi.org/10.1021/ja3102049

Sun J, Chen G, Wu J et al (2013a) Environmental bismuth vanadate hollow spheres: bubble template synthesis and enhanced photocatalytic properties for photodegradation. Appl Catal B Environ 132–133:304–314. https://doi.org/10.1016/j.apcatb.2012.12.002

Sun Y, Wang W, Sun S, Zhang L (2013b) A general synthesis strategy for one-dimensional Bi_2MO_6 (M = Mo, W) photocatalysts using an electrospinning method. CrystEngComm 15:7959–7964. https://doi.org/10.1039/c3ce41347k

Tang C, Zhang Y, Su J et al (2016) Synthesis and photocatalytic properties of vertically aligned Bi_2S_3 platelets. Solid State Sci 51:24–29. https://doi.org/10.1016/j.solidstatesciences.2015.11.004

Teweldebrhan D, Goyal V, Balandin AA (2010) Exfoliation and characterization of bismuth telluride atomic quintuples and quasi-two-dimensional crystals. Nano Lett 10:1209–1218. https://doi.org/10.1021/nl903590b

Tyagi M, Chatterjee R, Sharma P (2015) Structural, optical and ferroelectric behavior of pure $BiFeO_3$ thin films synthesized by the sol–gel method. J Mater Sci Mater Electron 26:1987–1992. https://doi.org/10.1007/s10854-014-2639-y

Venkatesan R, Velumani S, Ordon K et al (2018) Nanostructured bismuth vanadate ($BiVO_4$) thin films for efficient visible light photocatalysis. Mater Chem Phys 205:325–333. https://doi.org/10.1016/j.matchemphys.2017.11.004

Wang Y, Deng K, Zhang L (2011) Visible light photocatalysis of BiOI and its photocatalytic activity enhancement by in situ ionic liquid modification. J Phys Chem C 115:14300–14308. https://doi.org/10.1021/jp2042069

Wang H, Zhang L, Chen Z et al (2014) Semiconductor heterojunction photocatalysts: design, construction, and photocatalytic. Chem Soc Rev 43:5234–5244. https://doi.org/10.1039/c4cs00126e

Wang B, Yang H, Xian T et al (2015) Synthesis of spherical Bi_2WO_6 nanoparticles by a hydrothermal route and their photocatalytic properties. J Nanomater 2015. https://doi.org/10.1155/2015/146327

Wang K, Shao C, Li X, Miao F, Lu N, Liu Y (2016) Heterojunctions of p-BiOI Nanosheets/n-TiO2 nanofibers: preparation and enhanced visible-light photocatalytic activity. Materials 9(2):90

Wang Y, Long Y, Zhang D (2017) Facile in situ growth of high strong BiOI network films on metal wire meshes with photocatalytic activity. ACS Sustain Chem Eng. https://doi.org/10.1021/acssuschemeng.6b02810

Wang L, Liu J, Song W et al (2019a) Experimental and DFT insights of $BiVO_4$ as an effective photocatalytic catalyst for N_2O decomposition. Chem Eng J 366:504–513. https://doi.org/10.1016/j.cej.2019.02.038

Wang Z, Huang X, Wang X (2019b) Recent progresses in the design of $BiVO_4$-based photocatalysts for efficient solar water splitting. Catal Today. https://doi.org/10.1016/j.cattod.2019.01.067

Weidong H, Wei Q, Xiaohong W et al (2007) The photocatalytic properties of bismuth oxide films prepared through the sol–gel method. Thin Solid Films 515:5362–5365. https://doi.org/10.1016/j.tsf.2007.01.031

Wetchakun N, Chaiwichain S, Inceesungvorn B, Pingmuang K, Phanichphant S, Minett AI, Chen J (2012) BiVO/CeO nanocomposites with high visible-light-induced photocatalytic activity. ACS Appl Mater Interfaces 4(7):3718–3723

Wo B, Powers T, Haifeng C, Ting YAN (2013) Hydrothermal synthesis and photocatalytic properties of nano Bi_2WO_6/TiO_2 powers. Key Eng Mater:473–476. https://doi.org/10.4028/www.scientific.net/KEM.531-532.473

Wu T, Zhou X, Zhang H, Zhong X (2010) Bi_2S_3 nanostructures: a new photocatalyst. Nano Res 3:379–386. https://doi.org/10.1007/s12274-010-1042-0

Wu S, Wang C, Cui Y et al (2011) BiOCl nano/microstructures on substrates: synthesis and photocatalytic properties. Mater Lett 65(9):1344–1347

Xiaoxia LIU, Caimei FAN, Yunfang W et al (2012) Low temperature preparation of flower-like BiOCl film and its photocatalytic activity. Sci China Chem 55:2438–2444. https://doi.org/10.1007/s11426-012-4549-2

Xie H, Shen D, Wang X, Shen G (2008) Microwave hydrothermal synthesis and visible-light photocatalytic activity of γ-Bi_2MoO_6 nanoplates. Mater Chem Phys 110:332–336. https://doi.org/10.1016/j.matchemphys.2008.02.008

Xiong J, Cheng G, Li G et al (2011) Well-crystallized square-like 2D BiOCl nanoplates: mannitol-assisted hydrothermal synthesis and improved visible-light-driven photocatalytic performance. RSC Adv 1:1542–1553. https://doi.org/10.1039/c1ra00335f

Xiong J, Cheng G, Qin F et al (2013) Tunable BiOCl hierarchical nanostructures for high-efficient photocatalysis under visible light irradiation. Chem Eng J 220:228–236. https://doi.org/10.1016/j.cej.2013.01.033

Xu P, Shen X, Luo L, Shi Z, Liu Z, Chen Z, Zhu M, Zhang L (2018) Preparation of TiO/bi WO nanostructured heterojunctions on carbon fibers as a weaveable visible-light photocatalyst/photoelectrode. Environ Sci Nano 5(2):327–337

Yafei H, Zhang Y, Wang Y (2013) One-dimensional hierarchical Bi_2WO_6 hollow tubes with porous walls: synthesis and photocatalytic property. CrystEngComm 15:4124. https://doi.org/10.1039/C3CE40237A

Yan T, Sun M, Liu H, Wu T, Liu X, Yan Q, Xu W, Du B (2015) Fabrication of hierarchical BiOI/Bi2MoO6 heterojunction for degradation of bisphenol a and dye under visible light irradiation. J Alloys Compd 634:223–231

Yan L, Wang Y, Shen H, Zhang Y, Li J, Wang D (2017) Photocatalytic activity of Bi2WO6/Bi2S3 heterojunctions: the facilitation of exposed facets of Bi2WO6 substrate. Appl Surf Sci 393:496–503

Ye L, Deng K, Xu F et al (2012) Increasing visible-light absorption for photocatalysis with black BiOCl. Phys Chem Chem Phys 14:82–85. https://doi.org/10.1039/c1cp22876e

Yin W, Wang W, Sun S (2010a) Photocatalytic degradation of phenol over cage-like Bi_2MoO_6hollow spheres under visible-light irradiation. Catal Commun 11:647–650. https://doi.org/10.1016/j.catcom.2010.01.014

Yin W, Wang W, Zhou L et al (2010b) CTAB-assisted synthesis of monoclinic $BiVO_4$photocatalyst and its highly efficient degradation of organic dye under visible-light irradiation. J Hazard Mater 173:194–199. https://doi.org/10.1016/j.jhazmat.2009.08.068

Ying H, Chen W, Wen X et al (2018) Oxygen-deficient bismuth tungstate and bismuth oxide composite photoanode with improved photostability. Sci Bull:990. https://doi.org/10.1016/j.scib.2018.06.012

Yu J, Xiong J, Cheng B et al (2005) Hydrothermal preparation and visible-light photocatalytic activity of Bi_2WO_6 powders. J Solid State Chem 178:1968–1972. https://doi.org/10.1016/j.jssc.2005.04.003

Yu J, Wang S, Low J, Xiao W (2013) Enhanced photocatalytic performance of direct Z-scheme g-C_3N_4-TiO_2 photocatalysts for the decomposition of formaldehyde in air. Phys Chem Chem Phys 15:16883–16890. https://doi.org/10.1039/c3cp53131g

Yuxue Zhou PL (2017) CTAB-assisted fabrication of Bi_2WO_6 thin nanoplates with high adsorption and enhanced visible light-driven photocatalytic performance. Mol Artic. https://doi.org/10.3390/molecules22050859

Zargazi M, Entezari MH (2018) BFO thin film on the stainless steel mesh by anodic EPD: a visible light photocatalyst for degradation of Rhodamine B. J Photochem Photobiol A Chem 365:185–198. https://doi.org/10.1016/j.jphotochem.2018.07.042

Zargazi M, Entezari MH (2019a) A novel synthesis of forest like $BiFeO_3$ thin film: photo-electrochemical studies and its application as a photocatalyst for phenol degradation. Appl Surf Sci 483:793–802. https://doi.org/10.1016/j.apsusc.2019.03.347

Zargazi M, Entezari MH (2019b) Anodic electrophoretic deposition of Bi_2WO_6 thin film: high photocatalytic activity for degradation of a binary mixture. Appl Catal B Environ 242:507–517. https://doi.org/10.1016/j.apcatb.2018.09.093

Zargazi M, Entezari MH (2019c) Sonochemical versus hydrothermal synthesis of bismuth tungstate nanostructures: photocatalytic, sonocatalytic and sonophotocatalytic activities. Ultrason Sonochem 51:1–11. https://doi.org/10.1016/j.ultsonch.2018.10.010

Zhang C, Zhu Y (2005) Synthesis of square Bi_2WO_6 nanoplates as high-activity visible-light-driven photocatalysts. Chem Mater 17:3537–3545. https://doi.org/10.1021/cm0501517

Zhang K, Liu C, Huang F et al (2006) Study of the electronic structure and photocatalytic activity of the BiOCl photocatalyst. Appl Catal B Environ 68:125–129. https://doi.org/10.1016/j.apcatb.2006.08.002

Zhang L, Wang W, Zhou L, Xu H (2007) Bi_2WO_6 nano- and microstructures: shape control and associated visible-light-driven photocatalytic activities. Small 3:1618–1625. https://doi.org/10.1002/smll.200700043

Zhang X, Ai Z, Jia F, Zhang L (2008) Generalized one-pot synthesis, characterization, and photocatalytic activity of hierarchical BiOX (X = Cl, Br, I) nanoplate microspheres. J Phys Chem C 112:747–753. https://doi.org/10.1021/jp077471t

Zhang BLW, Wang YJ, Cheng HY et al (2009) Synthesis of porous Bi_2WO_6 thin films as efficient visible-light-active photocatalysts. Adv Mater 21:1286–1290. https://doi.org/10.1002/adma.200801354

Zhang L, Xu T, Zhao X, Zhu Y (2010) Controllable synthesis of Bi_2MoO_6 and effect of morphology and variation in local structure on photocatalytic activities. Appl Catal B Environ 98:138–146. https://doi.org/10.1016/j.apcatb.2010.05.022

Zhang H, Huang J, Zhou X, Zhong X (2011) Single-crystal Bi_2S_3 nanosheets growing via attachment-recrystallization of nanorods. Inorg Chem 50:7729–7734. https://doi.org/10.1021/ic201332n

Zhang D, Chen L, Xiao C et al (2016) Facile synthesis of high {001} facets dominated BiOCl nanosheets and their selective dye-sensitized photocatalytic activity induced by visible light. J Nanomater 2016. https://doi.org/10.1155/2016/5697672

Zhang J, Fu J, Wang Z, Cheng B, Dai K, Ho W (2018) Direct Z-scheme porous g-C3N4/BiOI heterojunction for enhanced visible-light photocatalytic activity. J Alloys Compd 766:841–850

Zhang Y, Shan G, Dong F et al (2019) Glass fiber supported BiOI thin-film fixed-bed photocatalytic reactor for water decontamination under solar light irradiation. J Environ Sci:1–10. https://doi.org/10.1016/j.jes.2019.01.004

Zhao H, Tian F, Wang R, Chen R (2014) A review on bismuth-related nanomaterials for photocatalysis. Rev Adv Sci Eng 3:3–27. https://doi.org/10.1166/rase.2014.1050

Zhou L, Wang W, Xu H et al (2009) Bi_2O_3 hierarchical nanostructures: controllable synthesis, growth mechanism, and their application in photocatalysis. Chem A Eur J 15:1776–1782. https://doi.org/10.1002/chem.200801234

Zhou Y, Meng X, Tong L et al (2016) Template-free fabrication of Bi_2WO_6 hierarchical hollow microspheres with visible-light-driven photocatalytic activity. Energies 9:764–775. https://doi.org/10.3390/en9100764

Zhu R, Tian F, Yang R et al (2019) Z Scheme system $ZnIn_2S_4$/RGO/$BiVO_4$ for hydrogen generation from water splitting and simultaneous degradation of organic pollutants under visible light. Renew Energy. https://doi.org/10.1016/j.renene.2019.02.049

Zhuo Y, Huang J, Cao L et al (2013) Photocatalytic activity of snow-like Bi_2WO_6 microcrystalline for decomposition of Rhodamine B under natural sunlight irradiation. Mater Lett 90:107–110. https://doi.org/10.1016/j.matlet.2012.09.009

Zong L, Cui P, Qin F et al (2017) Heterostructured bismuth vanadate multi-shell hollow spheres with high visible-light-driven photocatalytic activity. Mater Res Bull 86:44–50. https://doi.org/10.1016/j.materresbull.2016.09.031